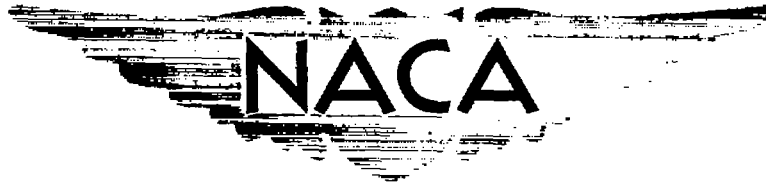


C. 12



RESEARCH MEMORANDUM

THE EFFECT OF LEADING-EDGE EXTENSIONS ON THE LONGITUDINAL CHARACTERISTICS AT MACH NUMBERS UP TO 0.92 OF A WING-FUSELAGE-TAIL COMBINATION HAVING A 40° SWEEPBACK WING WITH NACA 64A THICKNESS DISTRIBUTION

By Fred B. Sutton

Ames Aeronautical Laboratory
Moffett Field, Calif.

LIBRARY COPY

APR 10 1963

LANGLEY RESEARCH CENTER
LIBRARY, NACA
LANGLEY STATION
HAMPTON, VIRGINIA

CLASSIFIED DOCUMENT

This material contains information affecting the National Defense of the United States within the meaning of the espionage laws, Title 18, U.S.C., Secs. 793 and 794, the transmission or revelation of which in any manner to an unauthorized person is prohibited by law.

**NATIONAL ADVISORY COMMITTEE
FOR AERONAUTICS**

WASHINGTON

January 20, 1956

CLASSIFICATION CHANGED TO UNCLASSIFIED
AUTHORITY: NACA RESEARCH ABSTRACT NO. 120
EFFECTIVE DATE: SEPTEMBER 13, 1957
WHL



NATIONAL ADVISORY COMMITTEE FOR AERONAUTICS

RESEARCH MEMORANDUM

THE EFFECT OF LEADING-EDGE EXTENSIONS ON THE LONGITUDINAL
CHARACTERISTICS AT MACH NUMBERS UP TO 0.92 OF A WING-
FUSELAGE-TAIL COMBINATION HAVING A 40° SWEEPBACK
WING WITH NACA 64A THICKNESS DISTRIBUTION

By Fred B. Sutton

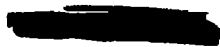
SUMMARY

A wind-tunnel investigation has been conducted to determine the effects of leading-edge extensions upon the longitudinal characteristics of a wing-fuselage and wing-fuselage-tail combination having a wing with 40° of sweepback and NACA 64A thickness distribution. The tests were made at a Mach number of 0.25 and a Reynolds number of 8 million and at Mach numbers varying from 0.25 to 0.92 at a Reynolds number of 2 million.

The addition of the leading-edge extension from 0.60 semispan to the wing tip eliminated large changes in longitudinal stability of the wing-fuselage-tail combination up to lift coefficients in excess of 1.0 at low speeds and resulted in slight increases in the lift coefficients at which large changes in stability occurred at high subcritical and supercritical speeds. In this regard, the chord extension was not so effective as the best combination of wing fences previously tested on this wing. The chord extension did not decrease the trim lift-drag ratios of the wing-fuselage-tail combination at high subcritical speeds and increased them slightly at supercritical speeds, whereas the fences caused about an 8-percent decrease in lift-drag ratio at Mach numbers from 0.70 to 0.86. As was the case with the wing fences, addition of the chord extension had only small effect on the Mach number for drag divergence. The leading-edge extensions had little effect on the tail contribution to stability at low speed and up to moderate lift coefficients at high speed.

INTRODUCTION

An investigation has been made in the Ames 12-foot pressure wind tunnel to determine the longitudinal characteristics of wings suitable for



long-range airplanes capable of moderately high subsonic speeds. Two twisted and cambered wings of relatively high aspect ratio, one having NACA four-digit and the other having NACA 64A thickness distribution, have been investigated with 40° , 45° , and 50° of sweepback, and the results are presented in reference 1. All of these wings experienced a severe decrease in longitudinal stability at moderate lift coefficients due to flow separation on the outer portions of the span. The results in references 2 and 3 show that the stability characteristics of these wings could be improved considerably by the use of multiple chordwise fences; however, the addition of fences resulted in moderate increases in drag for low to moderate lift coefficients at high subsonic speeds.

The present phase of the investigation was made to determine whether leading-edge extensions would improve the longitudinal stability characteristics of the wing with NACA 64A thickness distribution without the drag penalties associated with the fences. The wing with 40° of sweepback was tested in combination with a fuselage and with leading-edge extensions which were varied in spanwise extent. A comparison is made herein of the effect on the longitudinal characteristics of the model of a leading-edge extension and of the best arrangement of fences found in the investigation reported in reference 3. The wing-fuselage combination with a leading-edge extension was also tested with an all-movable horizontal tail to determine the effect of the leading-edge extension on the contribution of the tail to static-longitudinal stability and on the control effectiveness of the tail.

NOTATION

All wing areas and dimensions used in the notation refer to the unmodified wing.

A	aspect ratio, $\frac{b^2}{2S}$
a	mean-line designation, fraction of chord over which design load is uniform
a_t	lift-curve slope of the isolated horizontal tail, per deg
a_{w+f}	lift-curve slope of the wing-fuselage combination, per deg
a_{w+f+t}	lift-curve slope of the wing-fuselage-tail combination, per deg
$\frac{b}{2}$	wing semispan perpendicular to the plane of symmetry
C_D	drag coefficient, $\frac{\text{drag}}{qS}$

C_L	lift coefficient, $\frac{\text{lift}}{qS}$
C_m	pitching-moment coefficient about the quarter point of the wing mean aerodynamic chord, $\frac{\text{pitching moment}}{qS\bar{c}}$
c	local chord parallel to the plane of symmetry
c'	local chord perpendicular to the wing sweep axis
\bar{c}	mean aerodynamic chord, $\frac{\int_0^{b/2} c^2 dy}{\int_0^{b/2} c dy}$
c_{l_i}	section design lift coefficient
i_t	incidence of the horizontal tail with respect to the wing root chord
$\frac{L}{D}$	lift-drag ratio
M	free-stream Mach number
q	free-stream dynamic pressure
R	Reynolds number based on the wing mean aerodynamic chord
S	area of semispan wing
S_t	area of semispan horizontal tail
t	maximum thickness of section
y	lateral distance from the plane of symmetry
α	angle of attack, measured with respect to a reference plane through the leading edge and root chord of the wing
α_t	angle of attack of the isolated horizontal tail
ϵ	effective average downwash angle
ϕ	angle of twist, the angle between the local wing chord and the reference plane through the leading edge and the root chord of the wing (positive for washin and measured in planes parallel to the plane of symmetry)

η fraction of wing semispan, $\frac{y}{b/2}$

$\eta_t \left(\frac{q_t}{q} \right)$ tail efficiency factor (ratio of the lift-curve slope of the horizontal tail when mounted on the fuselage in the flow field of the wing to the lift-curve slope of the isolated horizontal tail)

Subscripts

f fuselage
t horizontal tail
w wing

MODEL

The wing-fuselage and wing-fuselage-tail combinations (fig. 1(a)) employed the twisted and cambered wing of reference 1 having the NACA 64A thickness distribution. For the unmodified wing, this distribution of thickness was combined with an $a = 0.8$ modified mean line having an ideal lift coefficient of 0.4 to form the sections perpendicular to the quarter-chord line of the unswept wing panel. The thickness-chord ratios of these sections varied from 14 percent at the root to 11 percent at the tip.

The chords of the leading-edge extensions were a constant percentage of the original chords and the extensions extended from either 45 percent of the span to the wing tip or from 60 percent of the span to the wing tip. The coordinates of the extensions were obtained by extending the wing sections perpendicular to the wing sweep axis forward 15 percent and modifying the mean line and thickness distribution of the sections as shown in figure 1(b). The extensions faired into the original wing at approximately 40 percent of the chord and were similar to the forward part of the original section except for reduced thickness ratio and nose radii. The reductions in nose radii amounted to approximately 23 percent. The inner faces of the extensions were parallel to the free stream and the extensions increased the wing area by either 4.6 or 6.3 percent.

The wing was constructed of solid steel and the surfaces were polished smooth. The leading-edge extensions were constructed of steel plates covered with a tin-bismuth alloy contoured to the desired section. For this investigation the angle of sweepback of the quarter-chord line of the unmodified wing was 40° and the aspect ratio of the unmodified wing was 7.0.

Twist was introduced by rotating the streamwise sections of the wing with 40° of sweepback about the original leading edge while maintaining the untwisted projected plan form. The variations of twist and thickness ratio along the semispan of the unmodified wing are shown in figure 1(c).

The fuselage employed for these tests consisted of a cylindrical mid-section with simple fairings fore and aft. Coordinates of the fuselage are listed in table I. The fuselage had a fineness ratio of 12.6 and was located with respect to the wing, so that the upper surface of the wing was nearly tangent to the top of the fuselage at the plane of symmetry. The angle of incidence of the wing root with respect to the fuselage center line was 3° . The fuselage shell was constructed of aluminum and was stiffened with a heavy steel structural member.

The all-movable horizontal tail had an aspect ratio of 3.0, a taper ratio of 0.5 and 40° of sweepback. The axis about which the incidence of the horizontal tail was varied was at 53.4 percent of the tail root chord. This hinge axis was at the intersection of the fuselage center line and the plane of the wing root chord (see fig. 1(a)). The tail was constructed of solid steel and the surfaces were polished smooth.

Figure 2 shows photographs of the model mounted in the wind tunnel and one of the leading-edge extensions. The turntable upon which the model was mounted is directly connected to the balance system.

CORRECTIONS TO DATA

The data have been corrected for constriction effects due to the presence of the tunnel walls by the method of reference 4, for tunnel-wall interference originating from lift on the model by the method of reference 5, and for drag tares caused by aerodynamic forces on the turntable upon which the model was mounted.

The corrections to dynamic pressure, Mach number, angle of attack, drag coefficient, and to pitching-moment coefficient were the same as those used for references 2 and 3 and are listed in table II.

RESULTS AND DISCUSSION

Tests were conducted to determine the longitudinal characteristics of the wing-fuselage combination with leading-edge chord extensions from 0.45 semispan to the wing tip and from 0.60 semispan to the wing tip. The results of these tests are shown in figures 3 through 10. Results of tests of the wing-fuselage-tail combination with wing leading-edge chord extensions are presented in figures 11 through 18.

Wing-Fuselage Combination

Figure 3 shows the effect of the leading-edge chord extensions on the longitudinal characteristics of the wing-fuselage combination at a Mach number of 0.25 and a Reynolds number of 8 million. The addition of the chord extensions increased the lift-curve slope in about the same proportion the wing area was increased and resulted in small increases in the lift coefficient at which large changes in static-longitudinal stability first occurred. The extension from 0.60 semispan to the tip reduced the magnitude of these stability changes at high lift coefficients. Figures 4 through 7 show the effect of the leading-edge extensions on the longitudinal characteristics of the wing-fuselage combination at Mach numbers up to 0.92 and at a Reynolds number of 2 million. As was the case at low speed and high Reynolds number, the extensions generally increased the lift-curve slopes at the higher lift coefficients (fig. 4) and lessened the severity of the changes in pitching moment with increasing lift coefficient (fig. 5). At most Mach numbers, the shorter chord extension, from 0.60 semispan to the tip, did not have much effect on the lift coefficient at which these changes occurred; however, the longer extension, 0.45 semispan to the tip, reduced the lift coefficient for instability at Mach numbers from 0.60 to 0.83. The effect of the leading-edge extensions on the drag and the lift-drag ratios of the combination are shown in figures 6 and 7, respectively. The extensions increased drag slightly at low and moderate lift coefficients, but reduced drag at the higher lift coefficients.

The effect of the leading-edge extension from 0.60 $b/2$ to the tip on the longitudinal characteristics of the combination are compared in figure 8 with the effect of the best arrangement of fences previously tested on this wing and reported in reference 3. Both devices increased the lift-curve slopes of the combination at high lift coefficients (fig. 8(a)). For the wing with leading-edge extensions these increases were due, at least in part, to the increased wing area. The addition of fences improved the stability of the combination to a much greater degree than did the leading-edge extension, both in regard to increasing the lift coefficient at which abrupt changes in stability occurred and in reducing the magnitude of these changes (fig. 8(b)). Drag penalties associated with the fences at low and moderate lift coefficients usually were slightly higher than those for the leading-edge extension (fig. 8(c)). This is shown more clearly by the lift-drag ratios which are compared in figure 8(d).

Effects of Mach number. - The effects of Mach number on the lift and pitching-moment curve slopes at a lift coefficient of 0.4 are shown in figure 9 for the wing-fuselage combination with the unmodified wing, the wing with leading-edge chord extensions, and the wing with the best fences found in the investigation reported in reference 3. The lift characteristics of the model with the leading-edge extensions or fences were less

affected by increasing Mach number than those of the combination with the unmodified wing; however, increasing Mach number caused more pronounced and varied changes in the stability of the combination with either leading-edge extension than for the combination with the unmodified wing or the wing with fences. Figure 10 shows the effect of Mach number on the drag coefficients of the wing-fuselage combination for several constant lift coefficients. The Mach numbers for drag divergence (defined as the Mach number at which $dC_D/dM = 0.10$) of the combination were only slightly affected by the addition of leading-edge extensions or wing fences. These values of drag-divergence Mach number and the corresponding drag coefficients are compared with those for the combination with the unmodified wing in the following tables:

C_L	M for drag divergence			
	Unmodified wing	Leading-edge extension from 0.45 b/2 to tip	Leading-edge extension from 0.60 b/2 to tip	Wing with fences
0.20	0.91	0.90	0.89	0.90
.40	.84	.86	.84	.86
.50	.82	.84	.82	.84
.60	.81	.82	.80	.82

C_L	$C_{D\text{divergence}}$			
	Unmodified wing	Leading-edge extension from 0.45 b/2 to tip	Leading-edge extension from 0.60 b/2 to tip	Wing with fences
0.20	0.0190	0.0185	0.0190	0.0200
.40	.0235	.0238	.0232	.0250
.50	.0265	.0292	.0273	.0295
.60	.0330	.0348	.0340	.0365

The effect of Mach number on the maximum lift-drag ratios and the lift coefficients for maximum lift-drag ratio are shown for the various wing modifications in figure 10.

Effects of Reynolds number.— A comparison of the data of figure 3 with the data in figures 4, 5, and 6 indicates that increasing Reynolds number from 2 million to 8 million had a large effect on the longitudinal characteristics of the wing-fuselage combination at a Mach number of 0.25. It is possible that the test results at higher Mach numbers may have been affected by the comparatively low Reynolds number (2 million) at which they were obtained. Caution should be exercised in applying these results to the prediction of the characteristics of a full-scale airplane.

Wing-Fuselage-Tail Combination

The wing-fuselage-tail combination was tested with both leading-edge extensions and the results are compared with those for the unmodified combination in figure 11. Figure 12 shows the effect of the leading-edge extensions on the pitching-moment contribution of the horizontal tail. Figures 13 and 14 summarize the effects of the extensions on the longitudinal characteristics of the model and compare these effects with those of the best arrangement of fences found in the investigation of reference 3. The cross plots in figures 13 and 14 are from the data presented in figures 11 and 15. Figure 15 shows, for several tail angles of incidence, the longitudinal characteristics of the model with the leading-edge extension from 0.60 semispan to the tip.

A comparison of the data in figures 8 and 11 shows that the effect of the extensions on the longitudinal characteristics of the wing-fuselage-tail combination was generally similar to the effect of the extensions on the model without the tail. At low speed and up to moderate lift coefficients at high speeds the extensions did not significantly affect the tail contribution to stability (fig. 12); however, the extensions, except at a Mach number of 0.80, increased the lift coefficient at which large changes in stability first occurred and reduced the magnitude of these changes at all Mach numbers (fig. 11).

Effects of Mach number.- Figure 13 shows the variation with Mach number of the slopes of the lift and pitching-moment curves of the wing-fuselage-tail combination with the unmodified wing, with chord extensions, and with the best fences reported in reference 3. The slope of the pitching-moment curve of the combination with either the chord extension or the fences appeared to be less affected by increasing Mach number than the slope for the model with the unmodified wing. The effect of Mach number on the drag coefficients of the combination with and without the extension from 0.60 semispan to the tip are shown in figure 14. Although the available data for the unmodified wing were meager, the extension had no apparent effect on the Mach numbers for drag divergence.

Lift-drag-ratio comparisons.- Figure 16 shows the variation with Mach number of the lift-drag ratio, the corresponding tail-incidence angle, and lift coefficient for a hypothetical airplane in level flight at 40,000 feet. Tail-incidence angles and lift-drag ratios are compared for the airplane with the unmodified wing of the subject investigation which used the NACA 64A thickness distribution, this wing with the leading-edge extension from 0.60 $b/2$ to the tip and this wing with its best fence arrangement (see ref. 3). Also included in this comparison are data from the investigation reported in reference 2. The model used in this investigation was similar to the model of the subject investigation except that the wing had the NACA four-digit thickness distribution. The results shown for this model are for the best arrangement of fences. It was

assumed that the airplane had a wing loading of 75 pounds per square foot and that the center of gravity was at the quarter point of the mean aerodynamic chord of the unmodified wing. It was also assumed that the airplane with the unmodified 64A wing trimmed at the same tail-incidence angles as with the 64A wing with fences. The lift-drag ratios of the airplane using the 64A wing with the extension from 0.60 semispan to the tip were equal at subcritical speeds to those of the airplane with the unmodified 64A wing and were slightly higher than those of the unmodified airplane at supercritical speeds; by comparison, the best arrangement of fences found in the investigation of reference 3 reduced the lift-drag ratio about 8 percent at Mach numbers from 0.70 to 0.86. It is of interest to note that at supercritical speeds, the combination using the four-digit wing with fences had higher lift-drag ratios than any of the 64A configurations. At least part of the lift-drag superiority of the combination using the 64A wing with the leading-edge extension or the four-digit wing with fences was due to the comparatively low tail-incidence angles required to trim these combinations.

Longitudinal characteristics of the wing-fuselage-tail combination.- The combination with the extension from 0.60 semispan to the tip was tested with a horizontal tail at several angles of incidence to determine the effect of the tail on the longitudinal characteristics and the effectiveness of the tail as a longitudinal control. The results of these tests are shown by the lift, drag, and pitching-moment data in figure 15. These data show that at most Mach numbers, the addition of the tail had only small effect on the lift and drag of the combination. The lift coefficients at which large changes in longitudinal stability first occurred were usually slightly larger with the tail than without it.

The factors which determine the tail contribution to the stability are shown in figure 17 as a function of angle of attack for several test conditions. The method used to calculate the effective downwash angle ϵ , the tail efficiency factor $\eta_t(q_t/q)$, and the ratio of the lift-curve slope for the isolated tail to the lift-curve slope of the wing-fuselage combination a_t/a_{w+t} was the same as that described in reference 2. The results of these calculations show that the reductions in pitching-moment variations at moderate lift coefficients with the tail on were mostly due to an increase in the factor a_t/a_{w+t} with increasing lift coefficient, in a manner which offset the reduction in stability of the wing-fuselage combination. This was true at most Mach numbers. At the higher lift coefficients and at a Reynolds number of 2 million, the rate of change of downwash with angle of attack and the tail efficiency factors were usually higher for the combination with the unmodified wing than for the combination with the extension. Figure 18 shows the variation with Mach number of the tail control effectiveness parameter $\partial C_m / \partial i_t$ and the factors affecting the stability contribution of the horizontal tail. Tail control effectiveness increased moderately with increasing Mach number and was slightly larger for the model with the unmodified wing than for the model with the leading-edge extension.

CONCLUSIONS

A wind-tunnel investigation has been made of a wing-fuselage and a wing-fuselage-tail combination having leading-edge extensions on a 40° sweptback wing. The unmodified wing had an aspect ratio of 7.0 and NACA 64A thickness distribution. The following conclusions were indicated:

1. The addition of a leading-edge extension from 0.60 semispan to the wing tip eliminated large changes in longitudinal stability of the wing-fuselage-tail combination up to lift coefficients in excess of 1.0 at low speeds and resulted in slight increases in the lift coefficients at which large changes in stability occurred at high subcritical and supercritical speeds. In this regard, the chord extension was not so effective as the best combination of wing fences previously tested on the wing.
2. The chord extension did not decrease the trim lift-drag ratios of the wing-fuselage-tail combination at high subcritical speeds and increased them slightly at supercritical speeds, whereas the fences caused about an 8-percent decrease in lift-drag ratio at Mach numbers from 0.70 to 0.86. As was the case with the wing fences, addition of the chord extension had only small effect on the Mach numbers for drag divergence.
3. The leading-edge extensions had little effect on the tail contribution to stability at low speed and at moderate lift coefficients at high speed.

Ames Aeronautical Laboratory
National Advisory Committee for Aeronautics
Moffett Field, Calif., Sept. 29, 1955

REFERENCES

1. Sutton, Fred B., and Dickson, Jerald K.: "A Comparison of the Longitudinal Aerodynamic Characteristics at Mach Numbers Up to 0.94 of Sweptback Wings Having NACA 4-Digit or NACA 64A Thickness Distributions." NACA RM A54E18, 1954.
2. Sutton, Fred B., and Dickson, Jerald K.: "The Longitudinal Characteristics at Mach Numbers Up to 0.92 of Several Wing-Fuselage-Tail Combinations Having Sweptback Wings With NACA Four-Digit Thickness Distributions." NACA RM A54L08, 1955.

3. Dickson, Jerald K., and Sutton, Fred B.: The Effect of Wing Fences on the Longitudinal Characteristics at Mach Numbers Up to 0.92 of a Wing-Fuselage-Tail Combination Having a 40° Sweptback Wing With NACA 64A Thickness Distribution. NACA RM A55C30a, 1955.
4. Herriot, John G.: Blockage Corrections for Three-Dimensional-Flow Closed-Throat Wind Tunnels, With Consideration of the Effect of Compressibility. NACA Rep. 995, 1950. (Formerly NACA RM A7B28)
5. Sivells, James C., and Salmi, Rachel M.: Jet-Boundary Corrections for Complete and Semispan Swept Wings in Closed Circular Wind Tunnels. NACA TN 2454, 1951.

TABLE I.- FUSELAGE COORDINATES

Distance from nose, in.	Radius, in.	Distance from nose, in.	Radius, in.
0	0	60.00	5.00
1.27	1.04	70.00	5.00
2.54	1.57	76.00	4.96
5.08	2.35	82.00	4.83
10.16	3.36	88.00	4.61
20.31	4.44	94.00	4.27
30.47	4.90	100.00	3.77
39.44	5.00	106.00	3.03
50.00	5.00	126.00	0

TABLE II.- CORRECTIONS TO DATA
(a) Corrections for constriction effects

Corrected Mach number	Uncorrected Mach number	$\frac{q_{corrected}}{q_{uncorrected}}$
0.25	0.250	1.003
.60	.599	1.006
.70	.696	1.007
.80	.793	1.010
.83	.821	1.012
.86	.848	1.015
.88	.866	1.017
.90	.883	1.020
.92	.899	1.024

(b) Corrections for tunnel-wall interference

$$\Delta\alpha = 0.455C_L$$

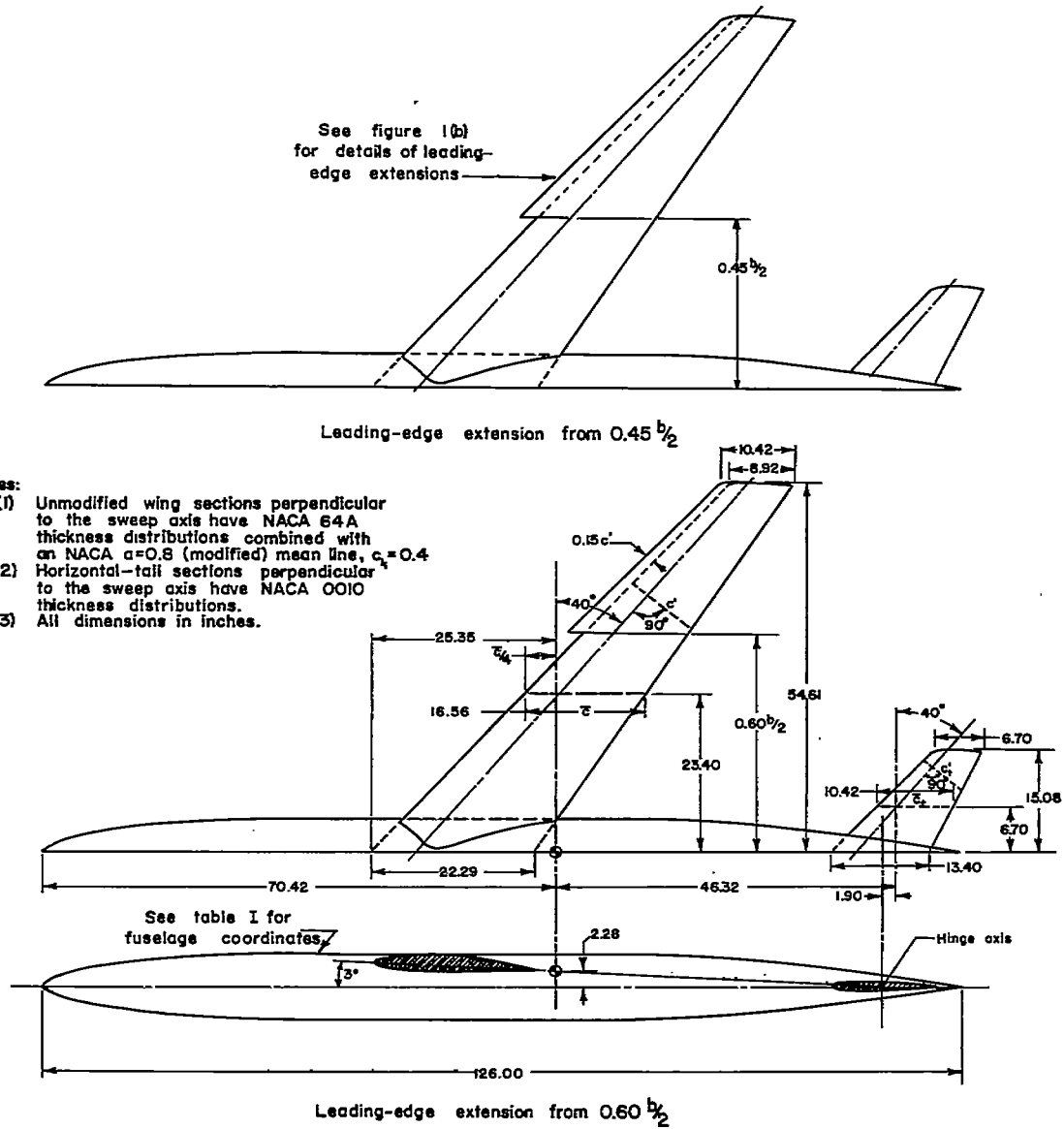
$$\Delta C_D = 0.00662C_L^2$$

$$\Delta C_{m \text{ tail off}} = K_1 C_{L \text{ tail off}}$$

$$\Delta C_{m \text{ tail on}} = K_1 C_{L \text{ tail off}} - \left[(K_2 C_{L \text{ tail off}} - \Delta\alpha) \frac{\partial C_m}{\partial i_t} \right]$$

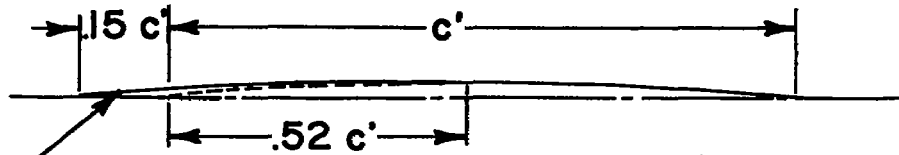
where:

M	K ₁	K ₂
0.25	0.0027	0.72
.60	.0038	.74
.70	.0043	.76
.80	.0049	.79
.83	.0050	.80
.86	.0053	.83
.88	.0054	.84
.90	.0056	.86
.92	.0057	.88



(a) Dimensions.

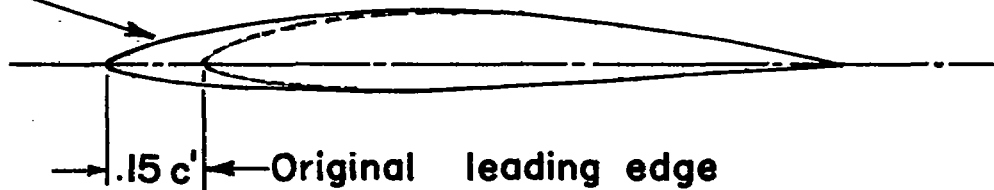
Figure 1.- Geometry of the model.



The mean line for the leading-edge extension ($a=0.8$, $c_i=0.31$) fairs into the original mean line ($a=0.8$, $c_i=0.4$) at the point of zero slope.

Mean-line modification

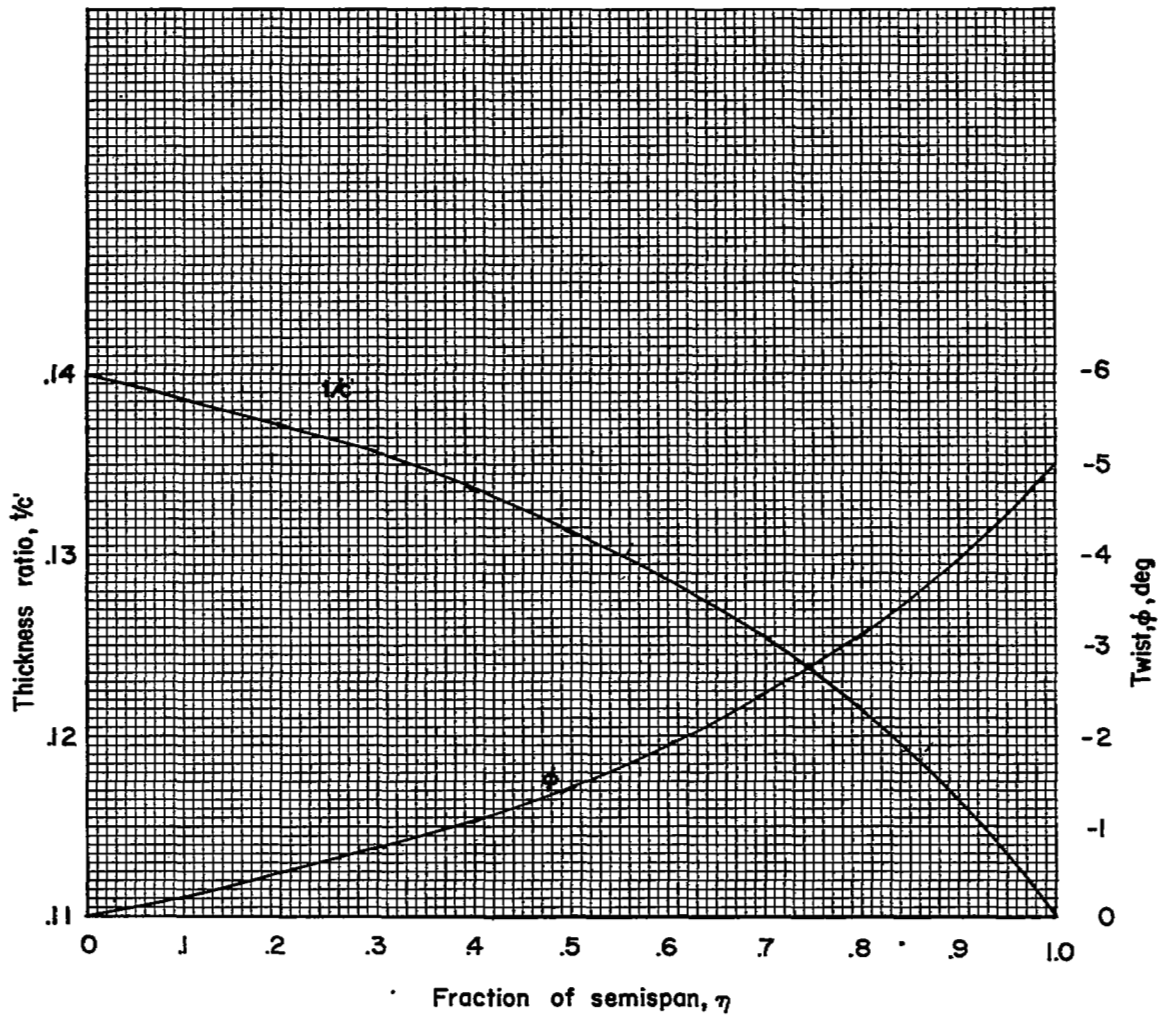
Profiles for the leading-edge extensions fair into the original wing at approximately 40 percent of the original chord and are similar to the forward portion of the original section except for reduced thickness ratio and leading-edge radii.



Typical modified section

(b) Details of leading-edge extension.

Figure 1.- Continued.



(c) Distribution of twist and thickness ratio.

Figure 1.- Concluded.



A-20146



A-20147

Figure 2.- Photographs of the model.

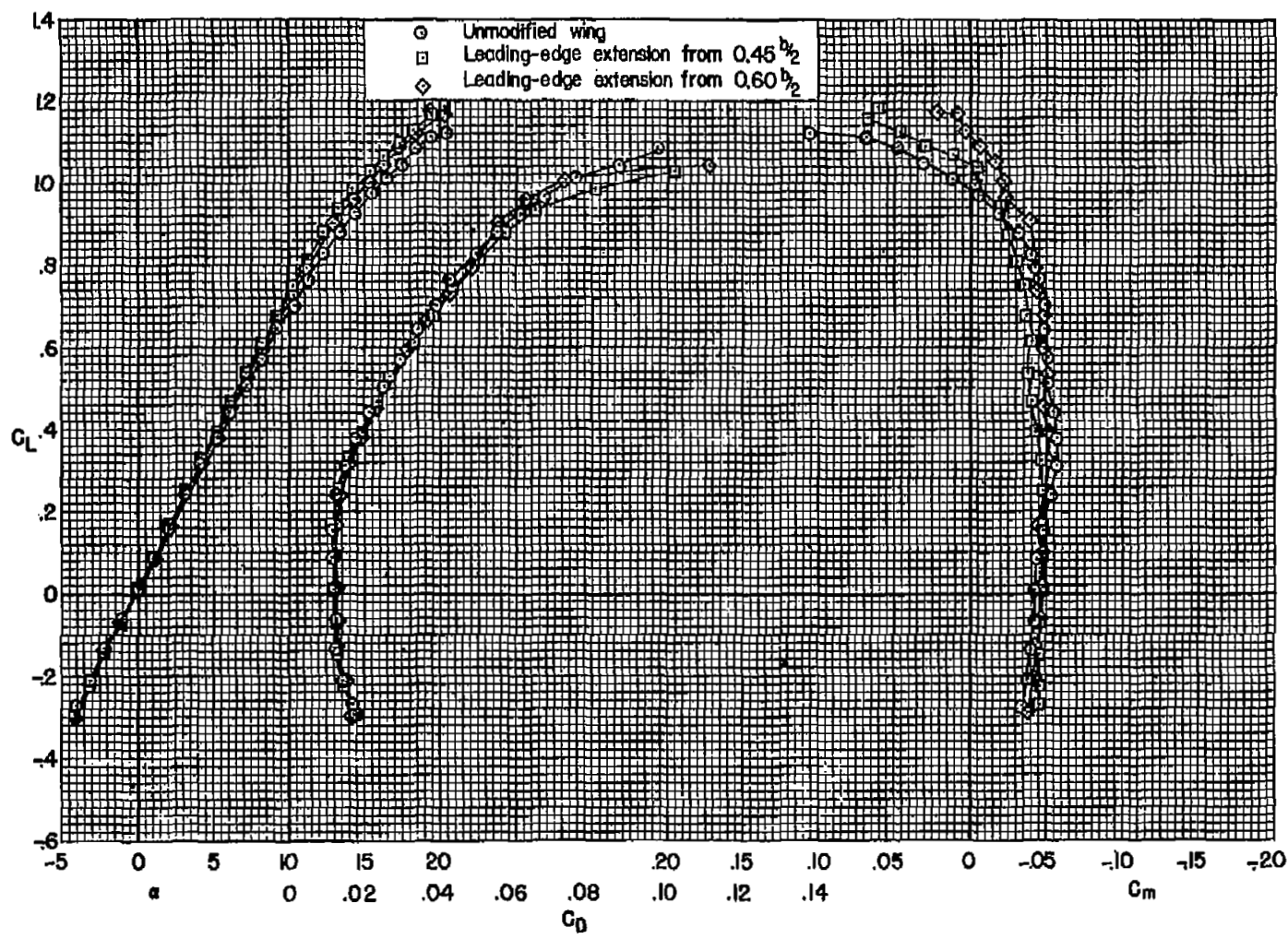
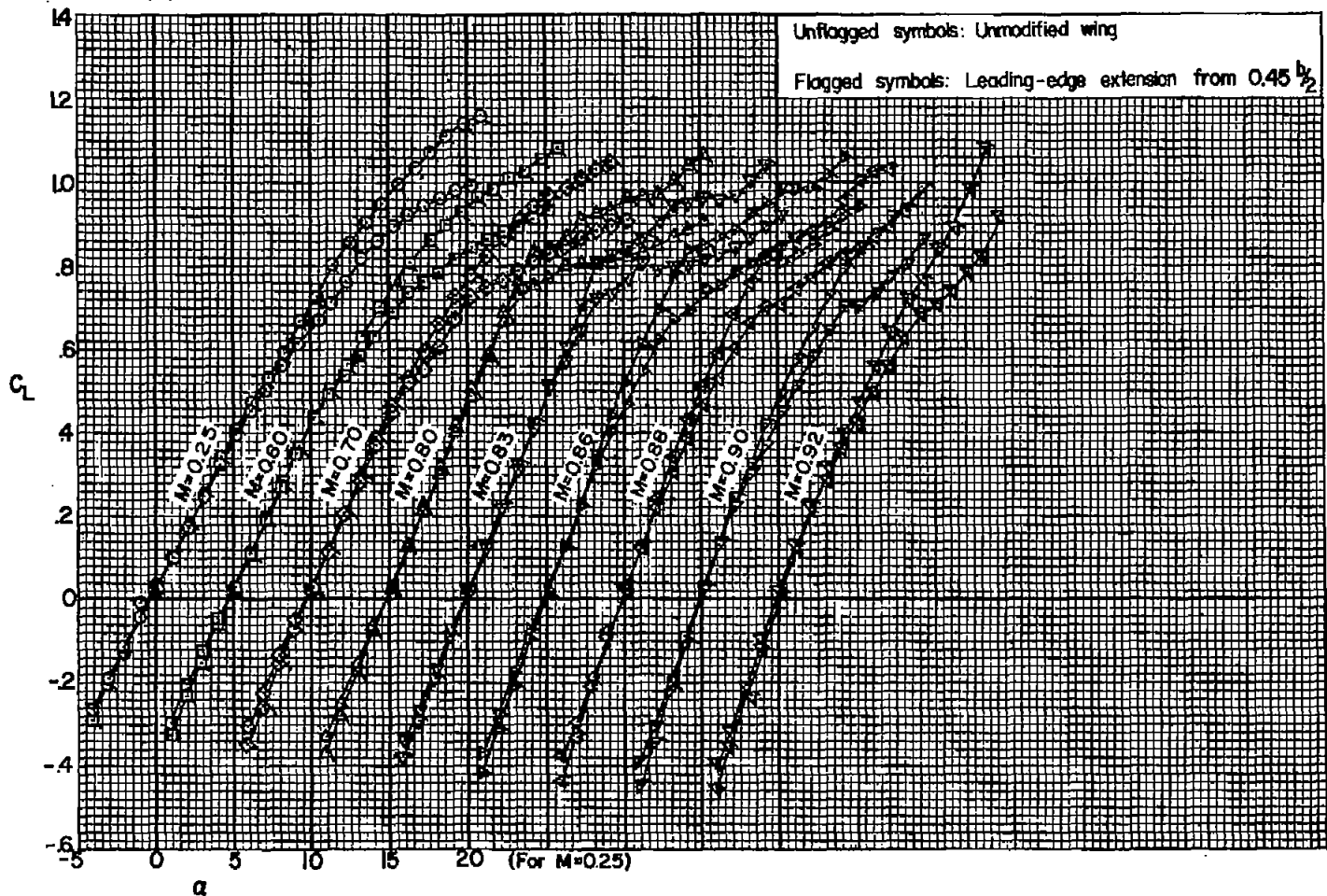
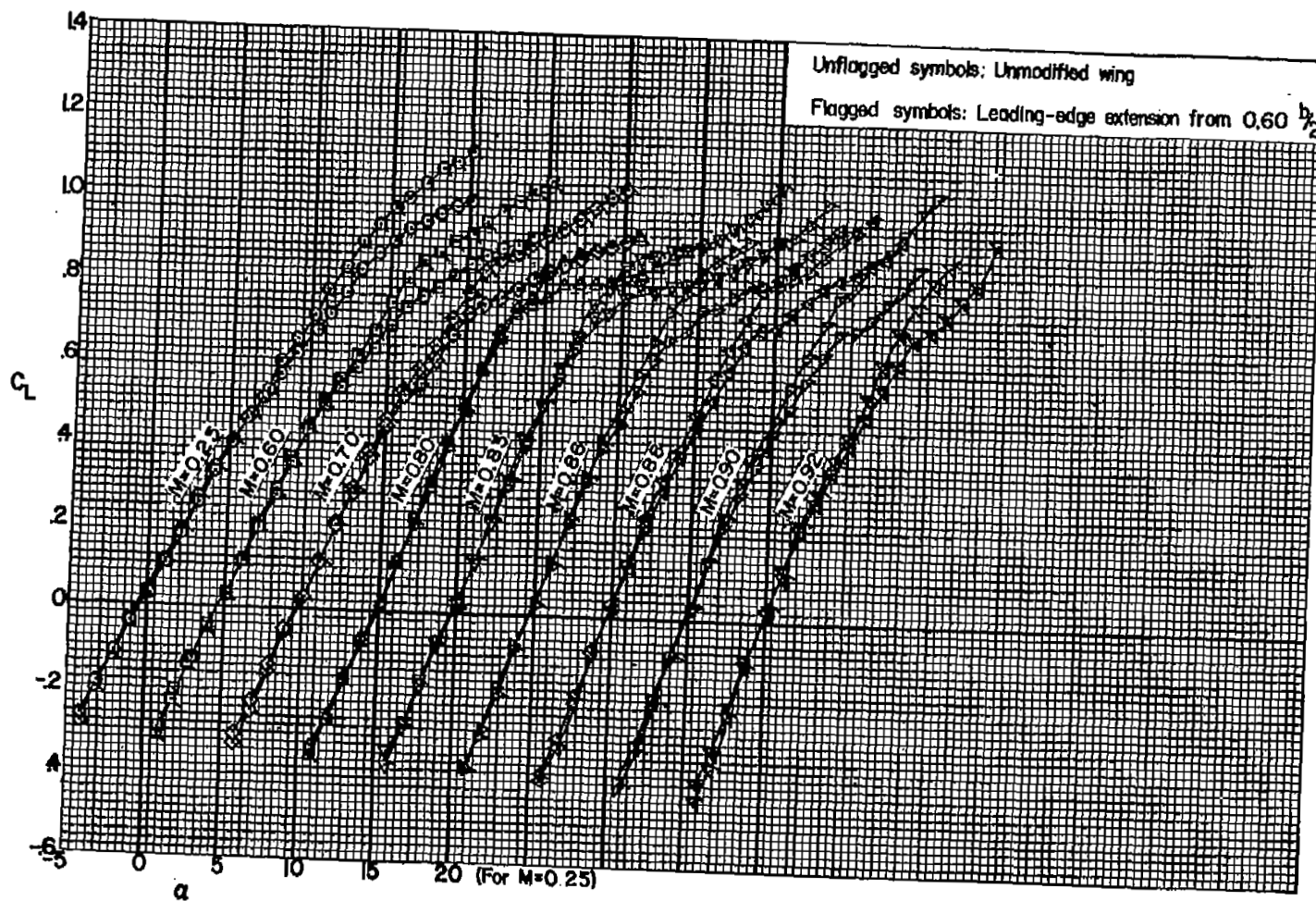


Figure 3.- The effect of leading-edge extensions on the longitudinal characteristics of the wing-fuselage combination; $M = 0.25$, $R = 8,000,000$.



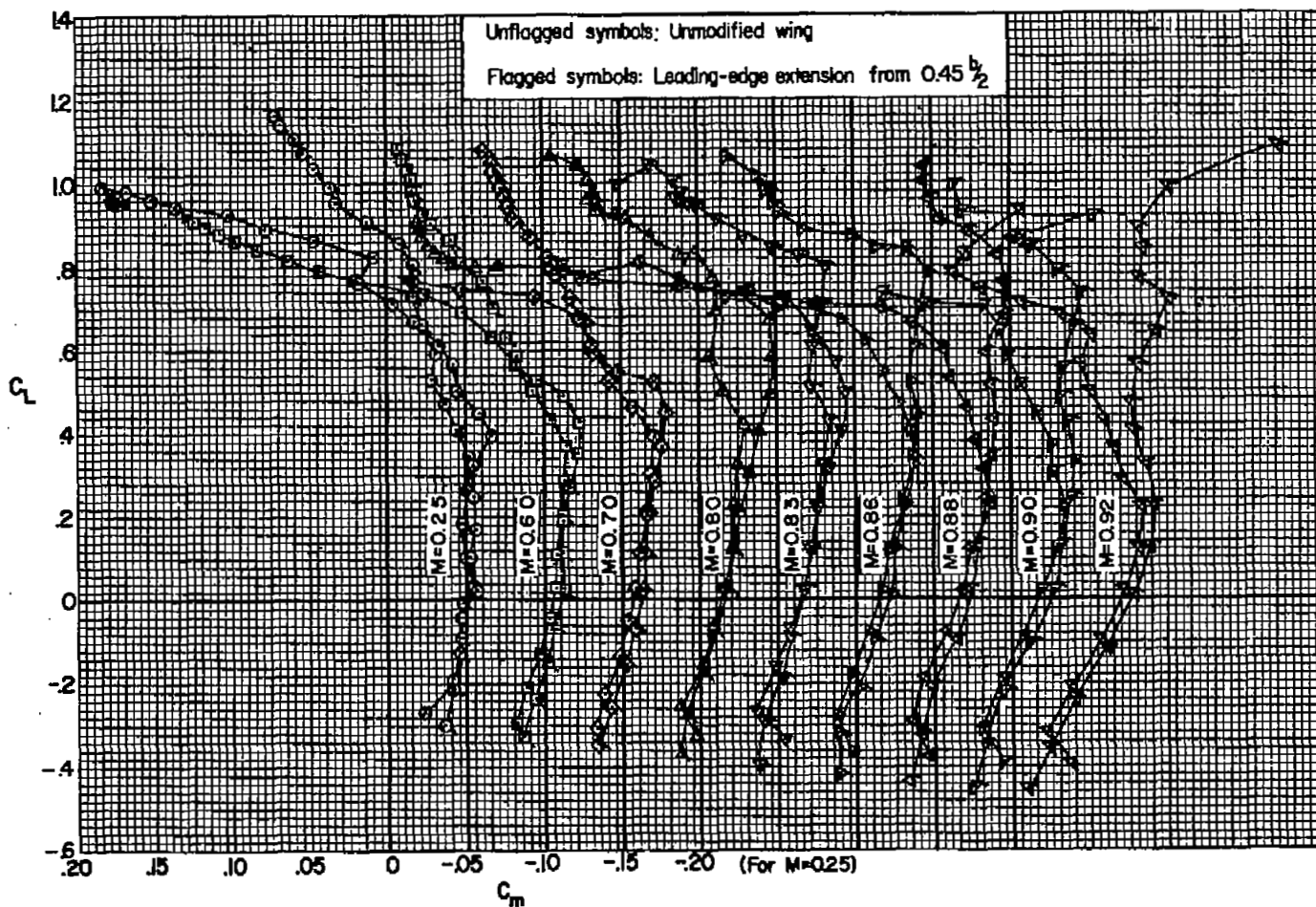
(a) Leading-edge extension from $0.45 \frac{b}{2}$ to tip.

Figure 4.- The effect of leading-edge extensions on the lift characteristics of the wing-fuselage combination at several Mach numbers; $R = 2,000,000$.



(b) Leading-edge extension from $0.60 b/2$ to tip.

Figure 4.- Concluded.



(a) Leading-edge extension from $0.45 \frac{b}{2}$ to tip.

Figure 5.- The effect of leading-edge extensions on the pitching-moment characteristics of the wing-fuselage combination at several Mach numbers; $R = 2,000,000$.

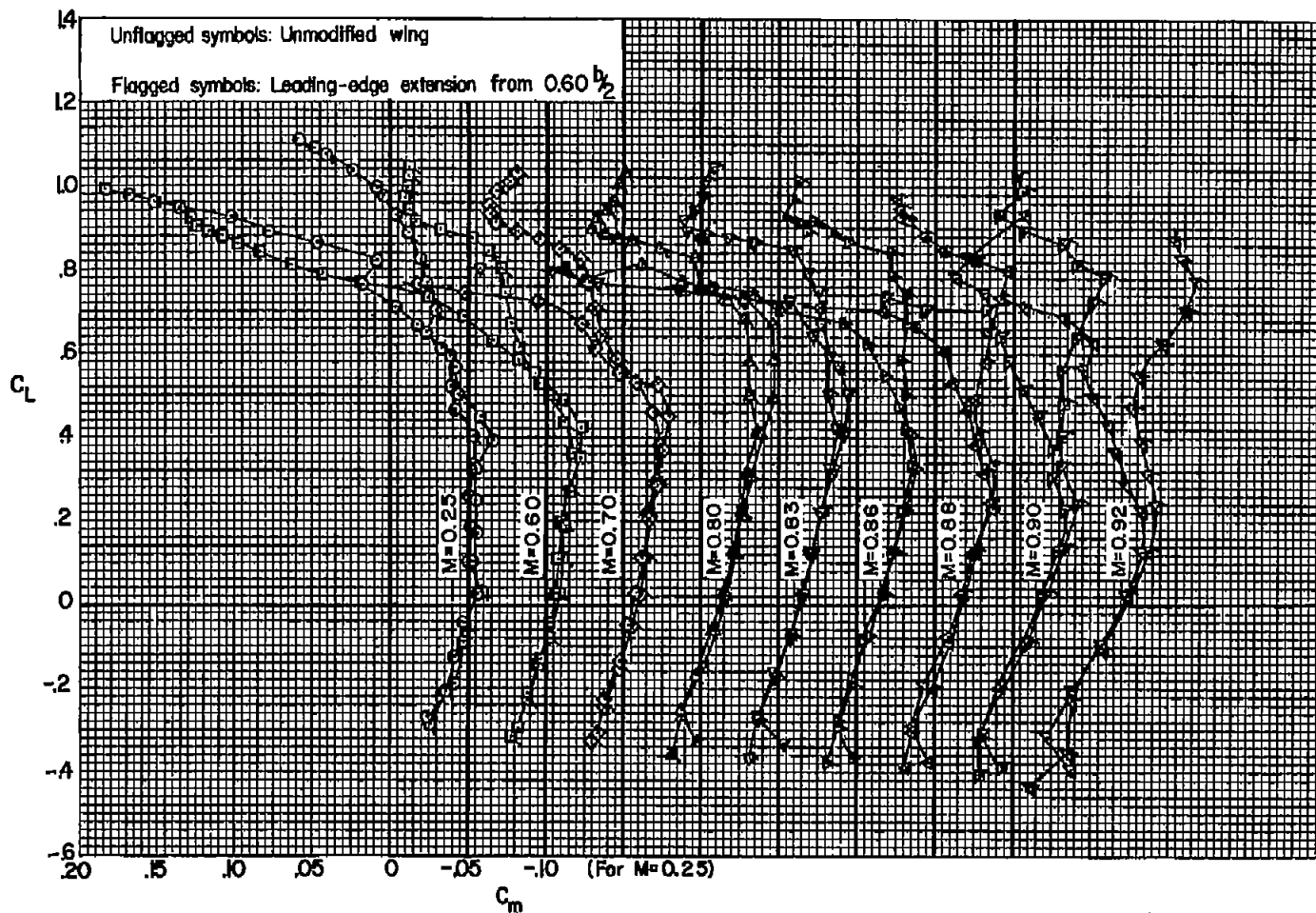
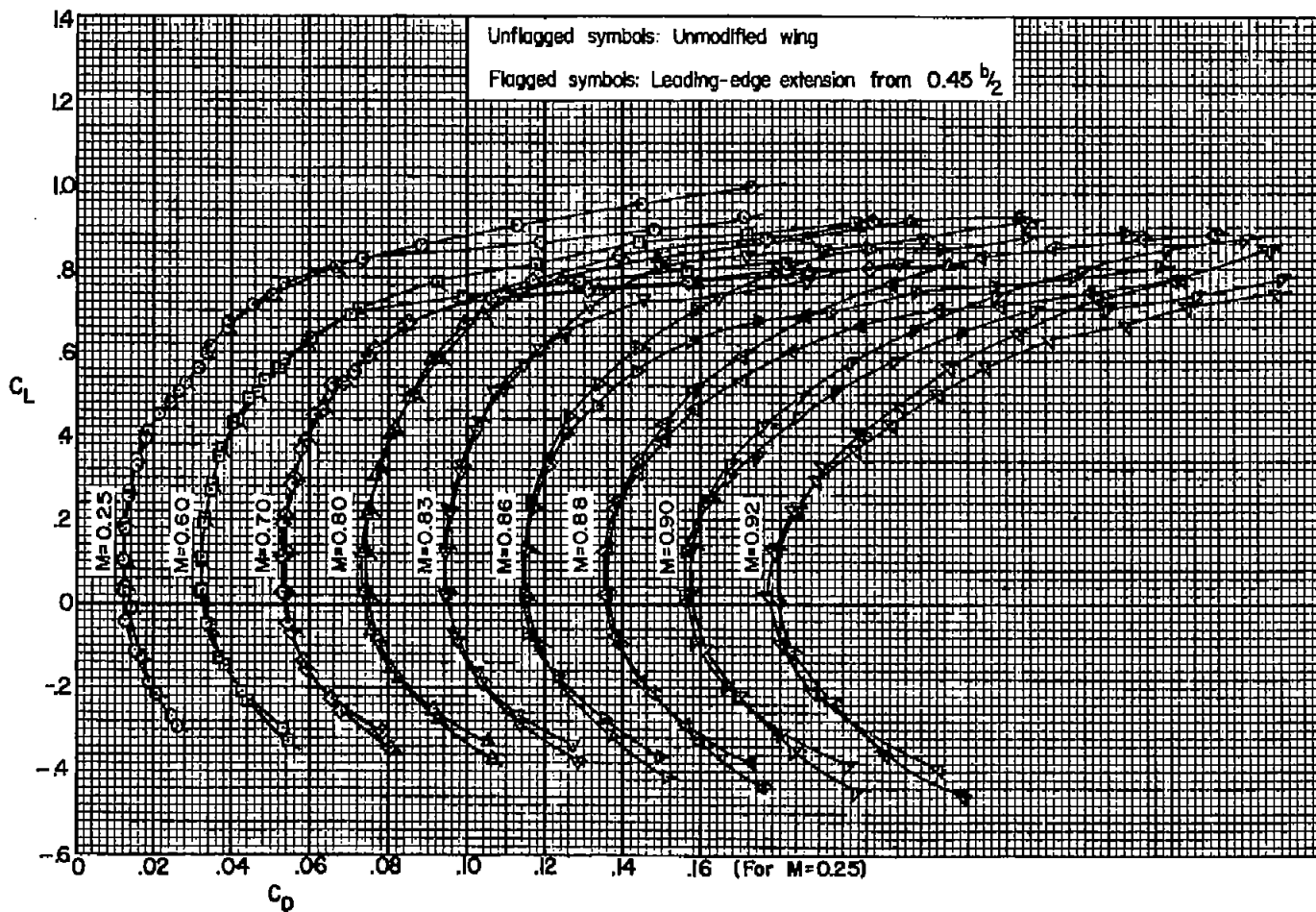
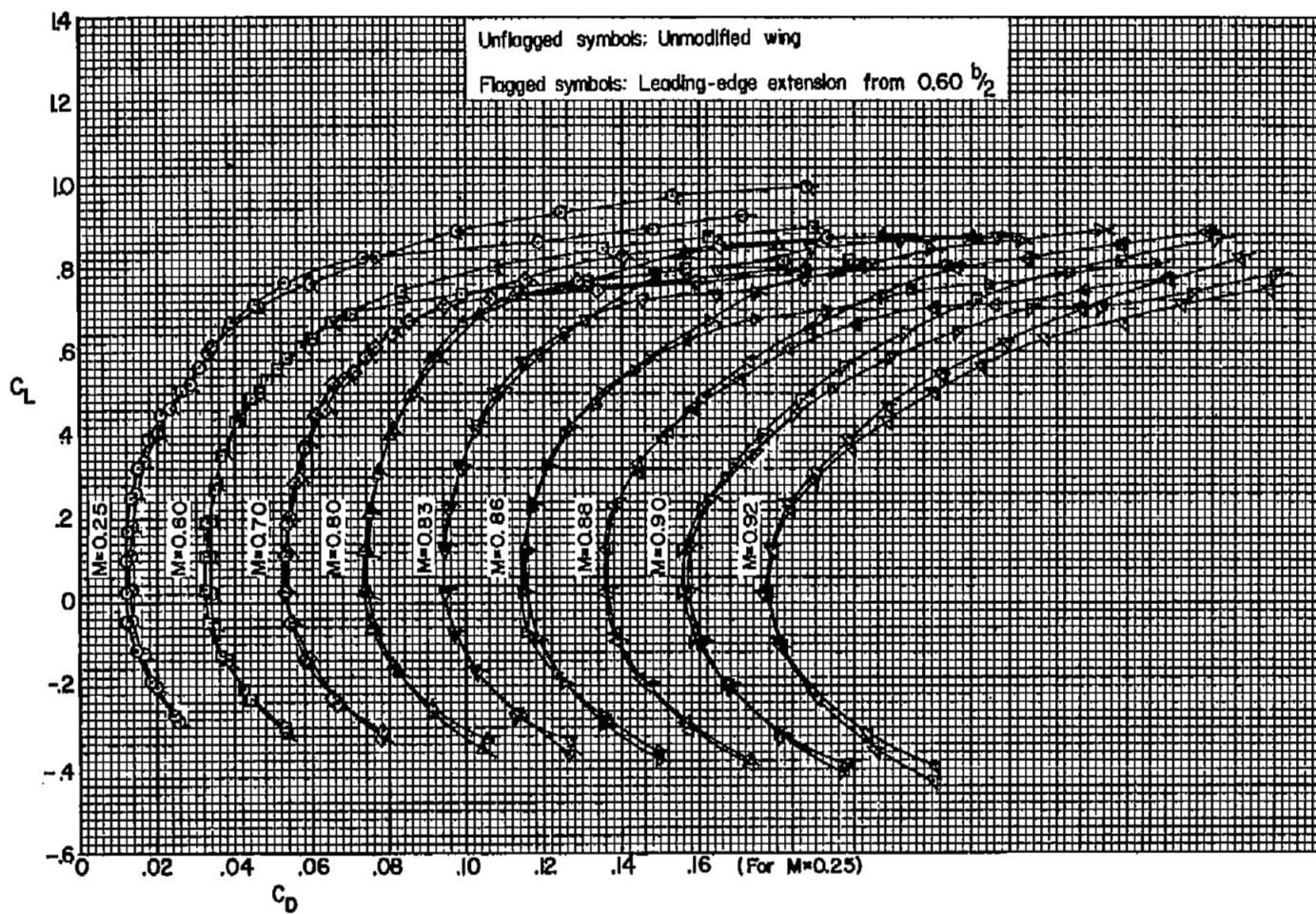
(b) Leading-edge extension from $0.60 b/2$ to tip.

Figure 5.- Concluded.



(a) Leading-edge extension from $0.45 b/2$ to tip.

Figure 6.- The effect of leading-edge extensions on the drag characteristics of the wing-fuselage combination at several Mach numbers; $R = 2,000,000$.



(b) Leading-edge extension from $0.60 \frac{b}{2}$ to tip.

Figure 6.- Concluded.

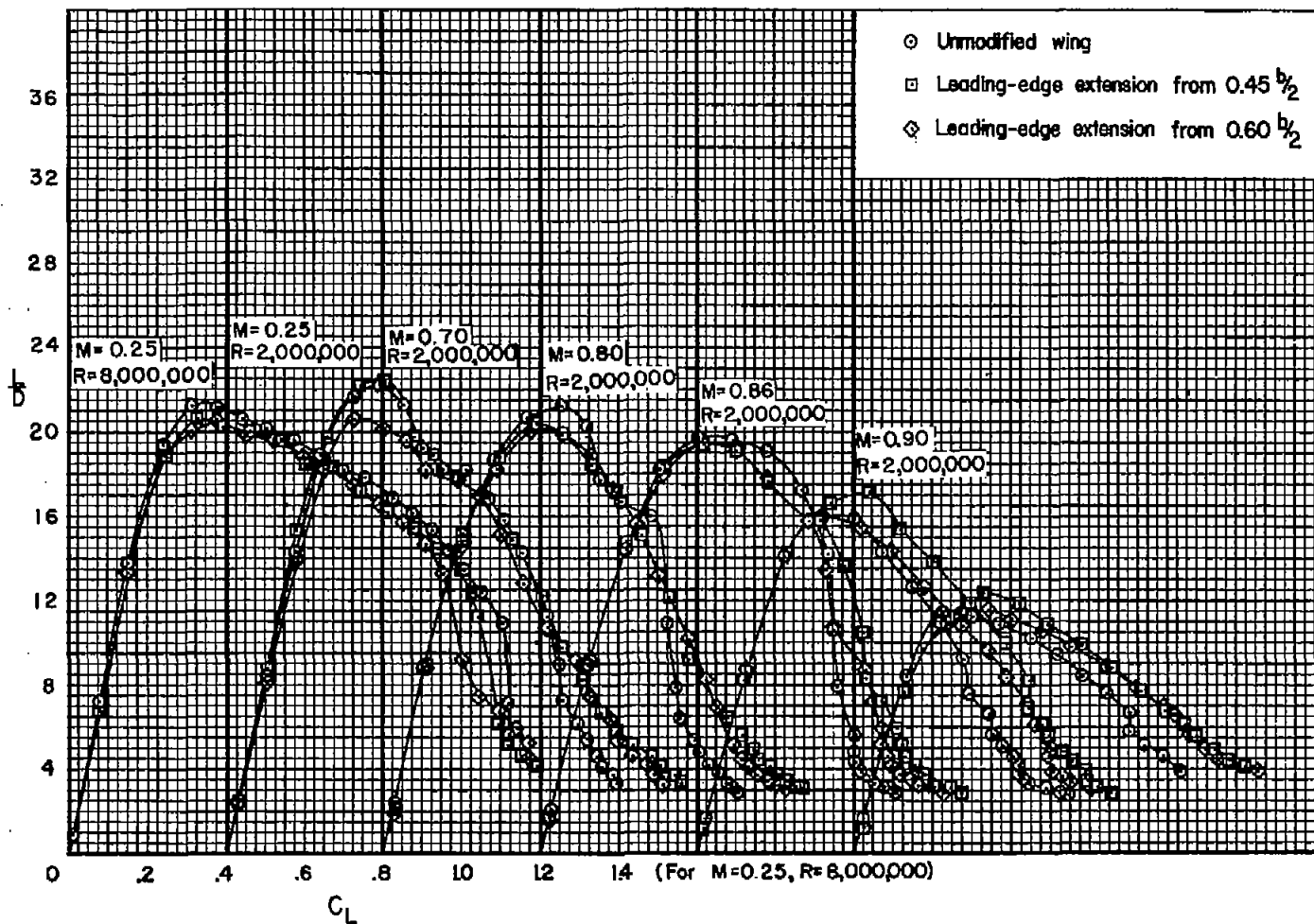
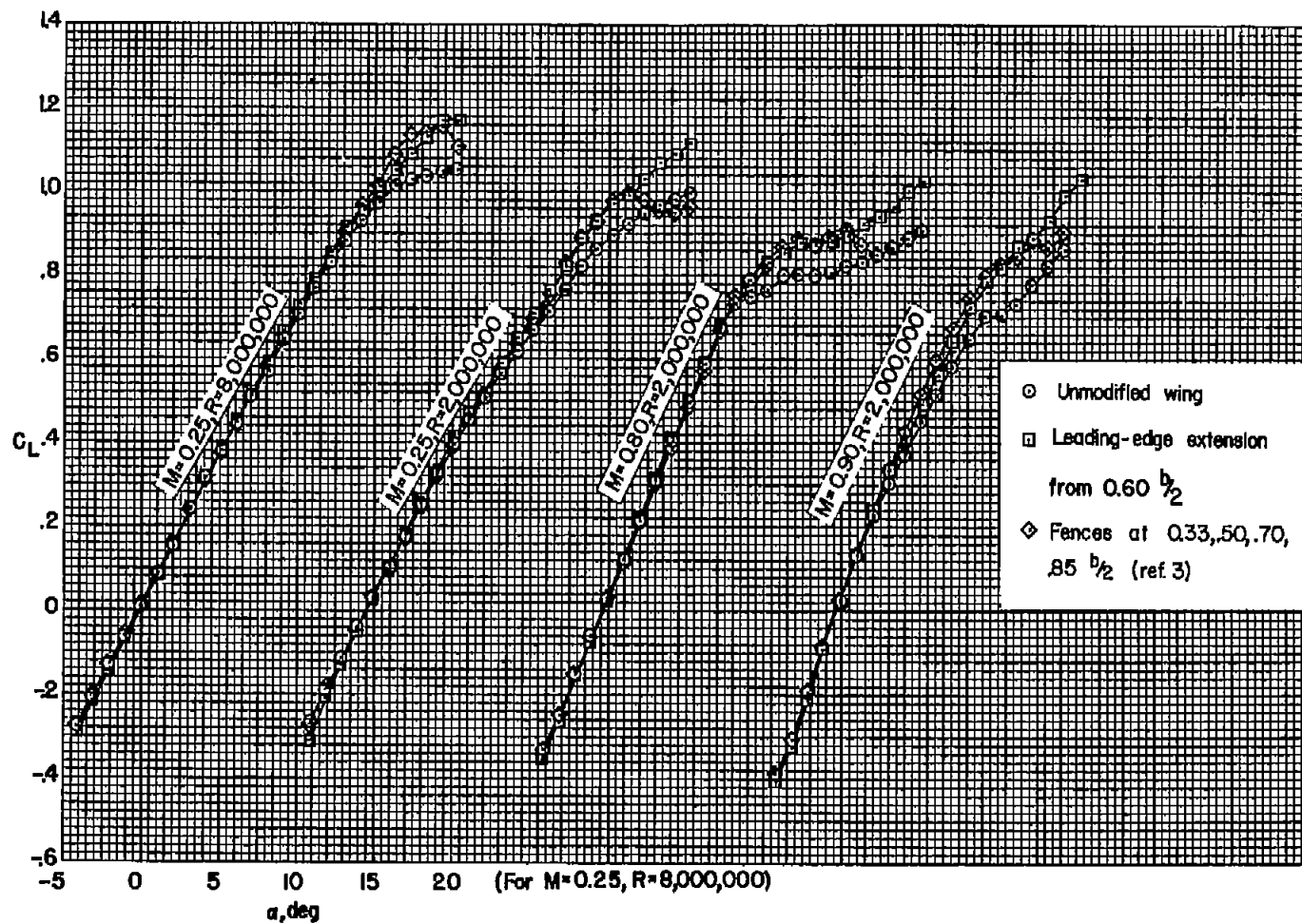
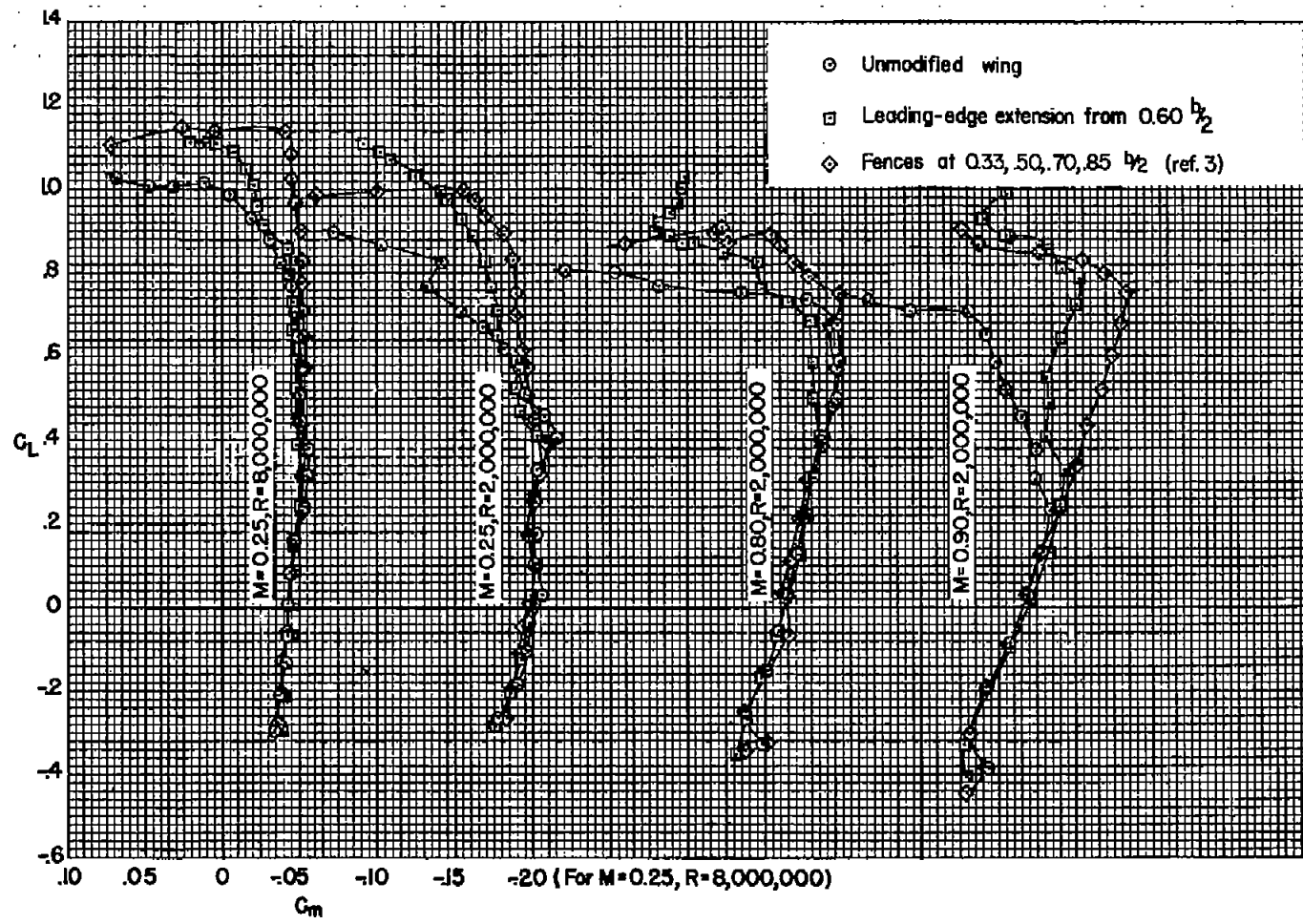


Figure 7.- The effect of leading-edge extensions on the lift-drag ratios of the wing-fuselage combination at several Mach numbers.



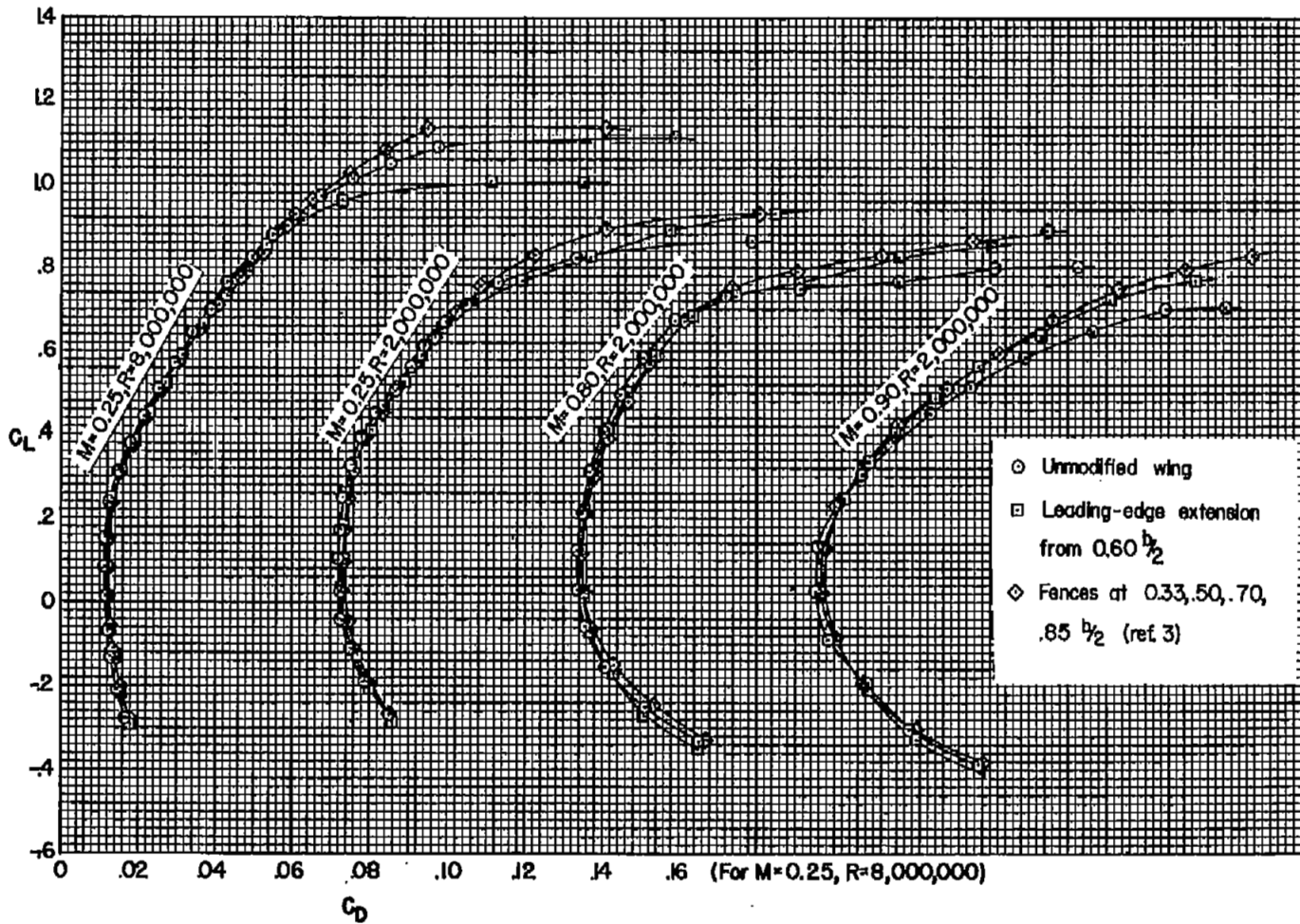
(a) Lift.

Figure 8.- Comparison of the effect of a leading-edge extension and wing fences on the longitudinal characteristics of the wing-fuselage combination.



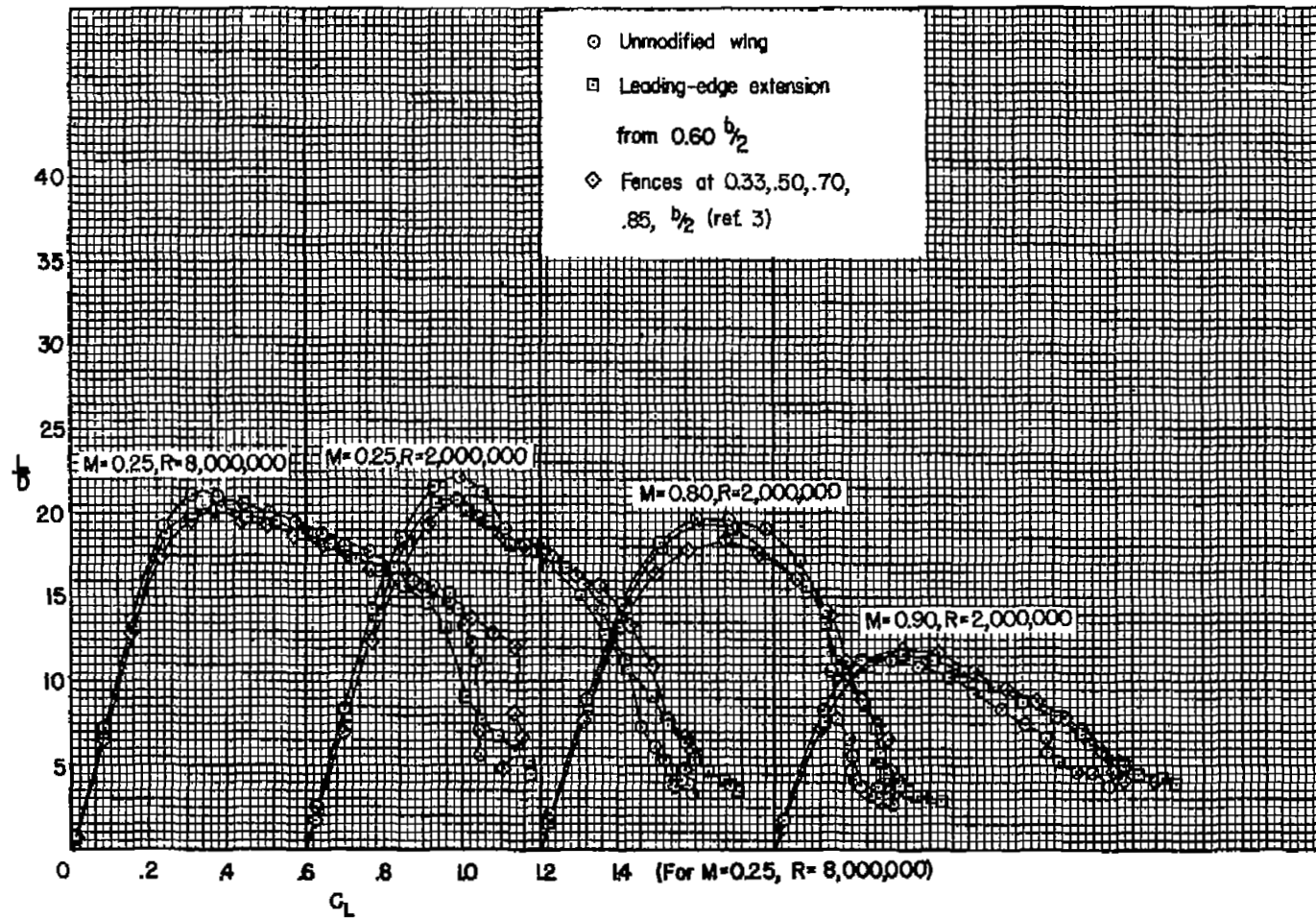
(b) Pitching moment.

Figure 8.- Continued.



(c) Drag.

Figure 8.- Continued.



(d) Lift-drag ratio.

Figure 8.- Concluded.

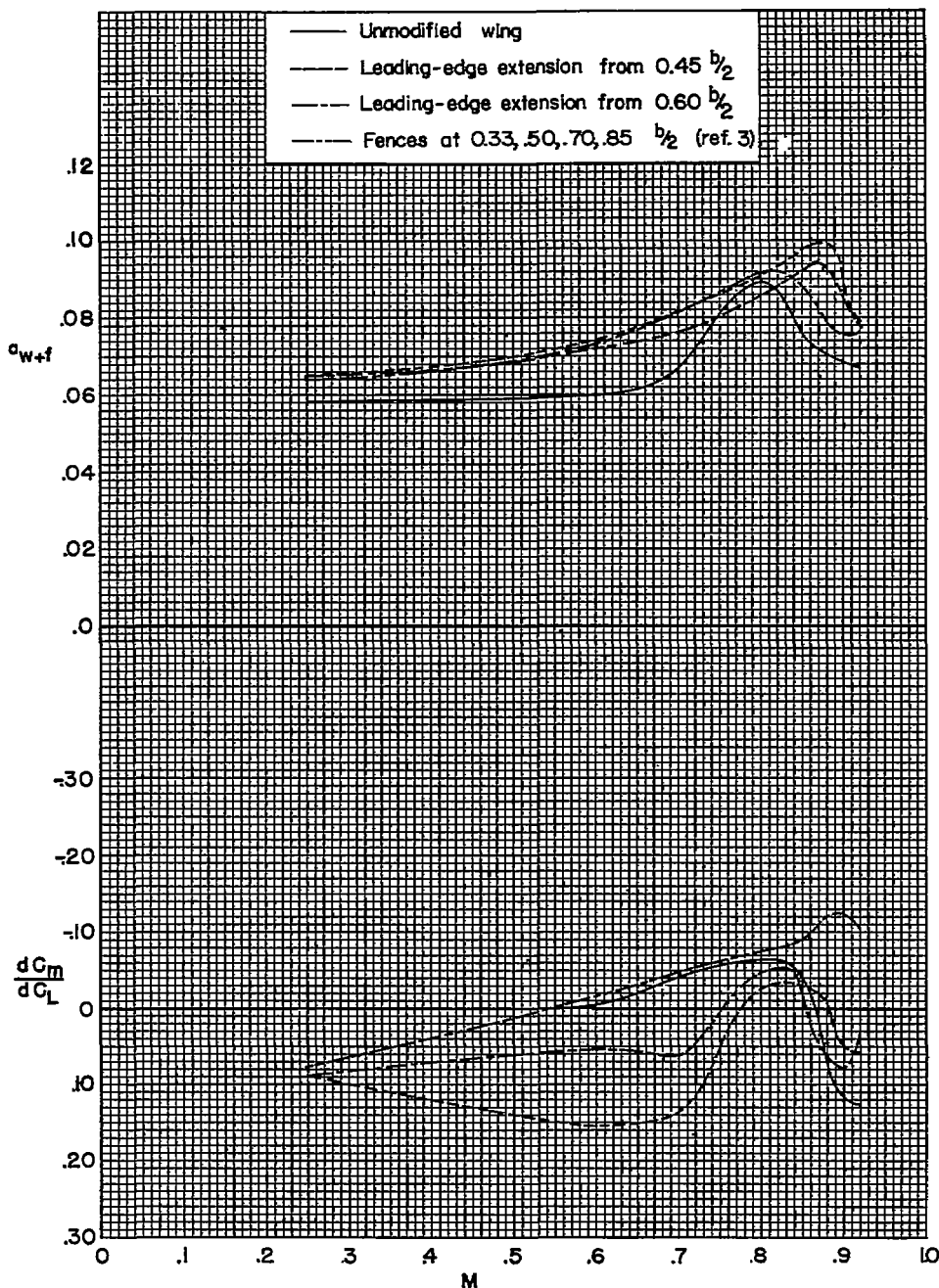


Figure 9.- The variation with Mach number of the slopes of the lift and pitching-moment curves of the wing-fuselage combination with and without leading-edge extensions and wing fences; $C_L = 0.40$, $R = 2,000,000$.

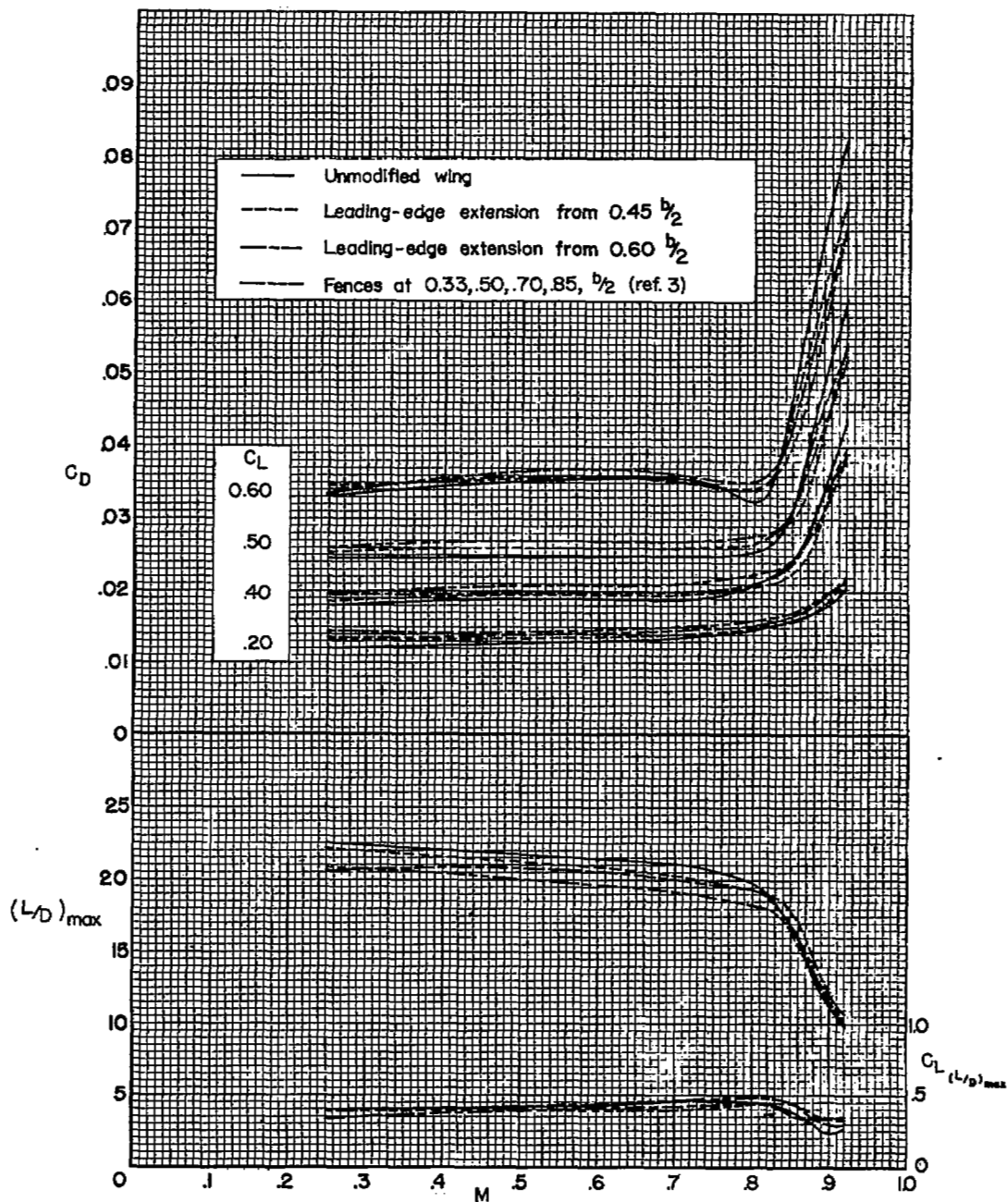
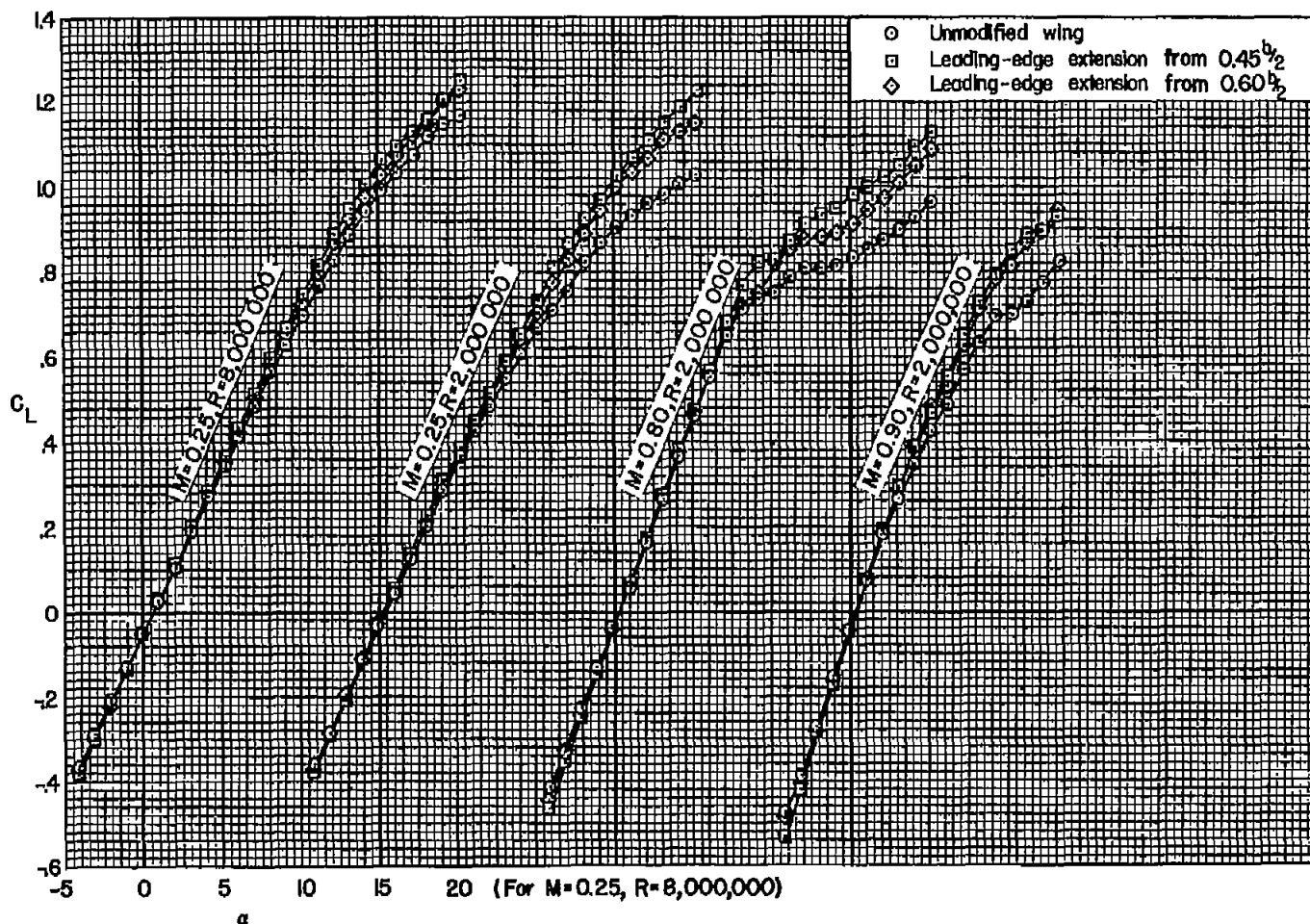
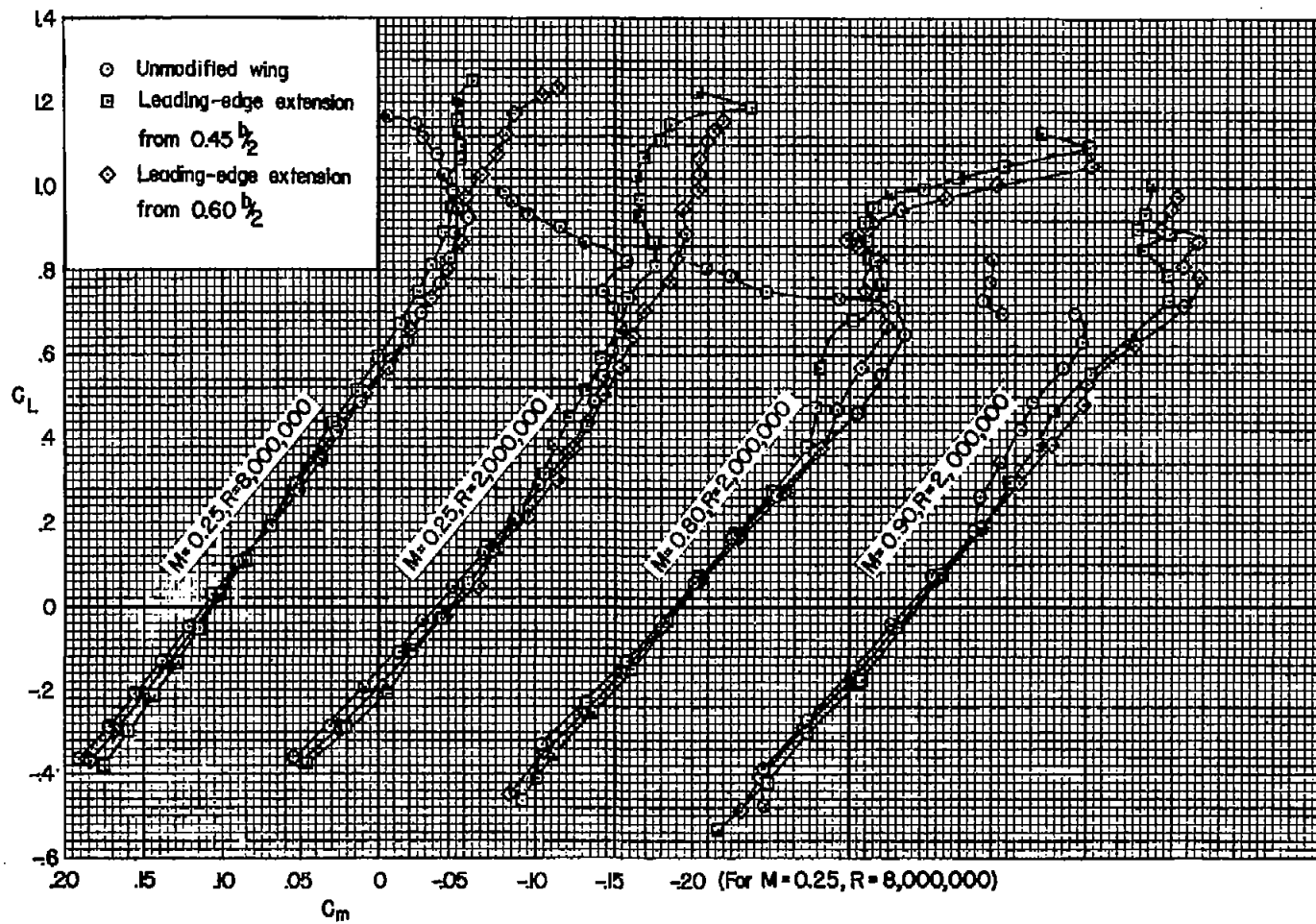


Figure 10.- The variation with Mach number of the drag coefficients and the maximum lift-drag ratios of the wing-fuselage combination with and without leading-edge extensions and wing fences; $R = 2,000,000$.



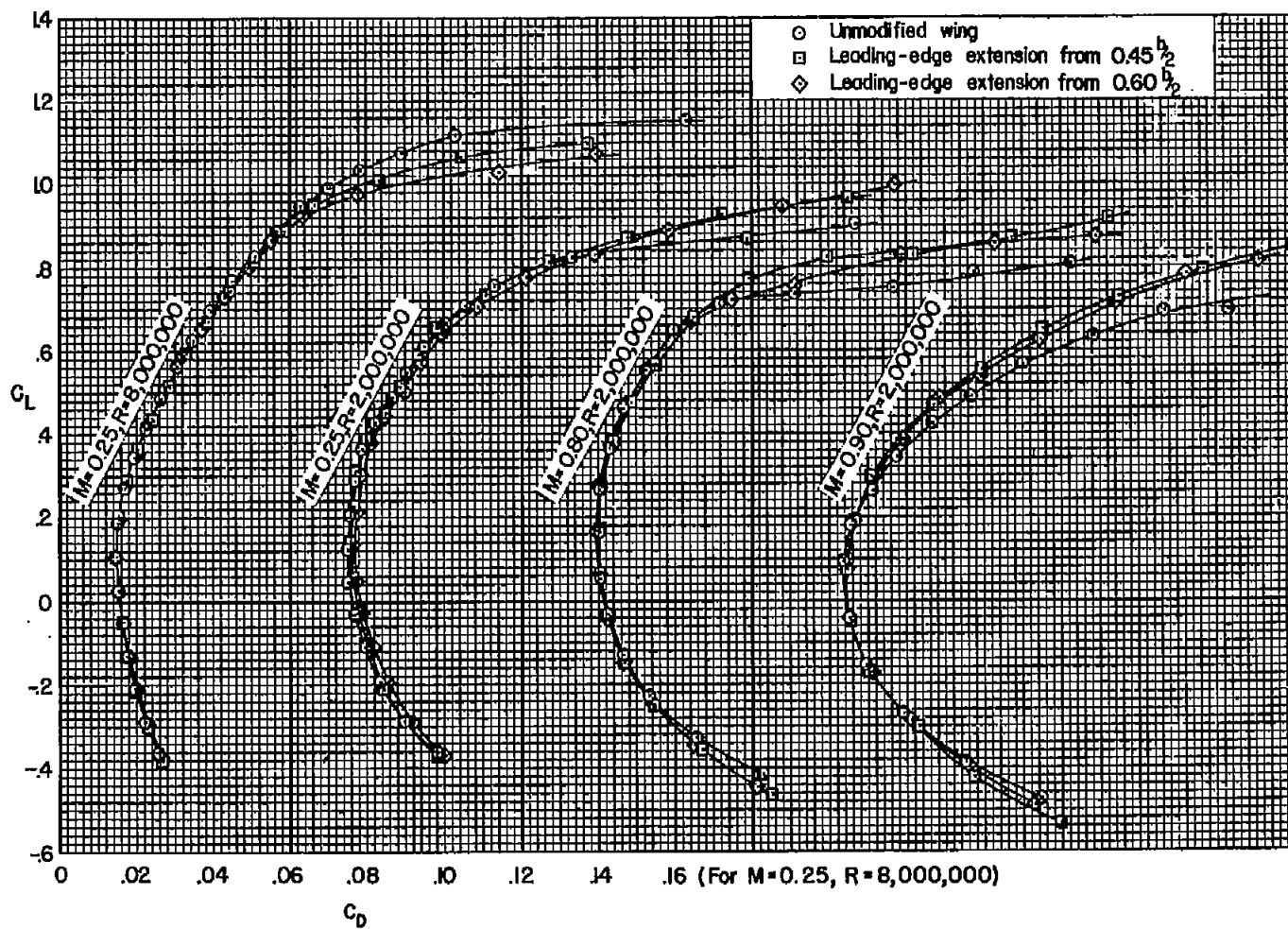
(a) Lift.

Figure 11.- The effect of leading-edge extensions on the longitudinal characteristics of the wing-fuselage-tail combination; $i_t = -8^\circ$.



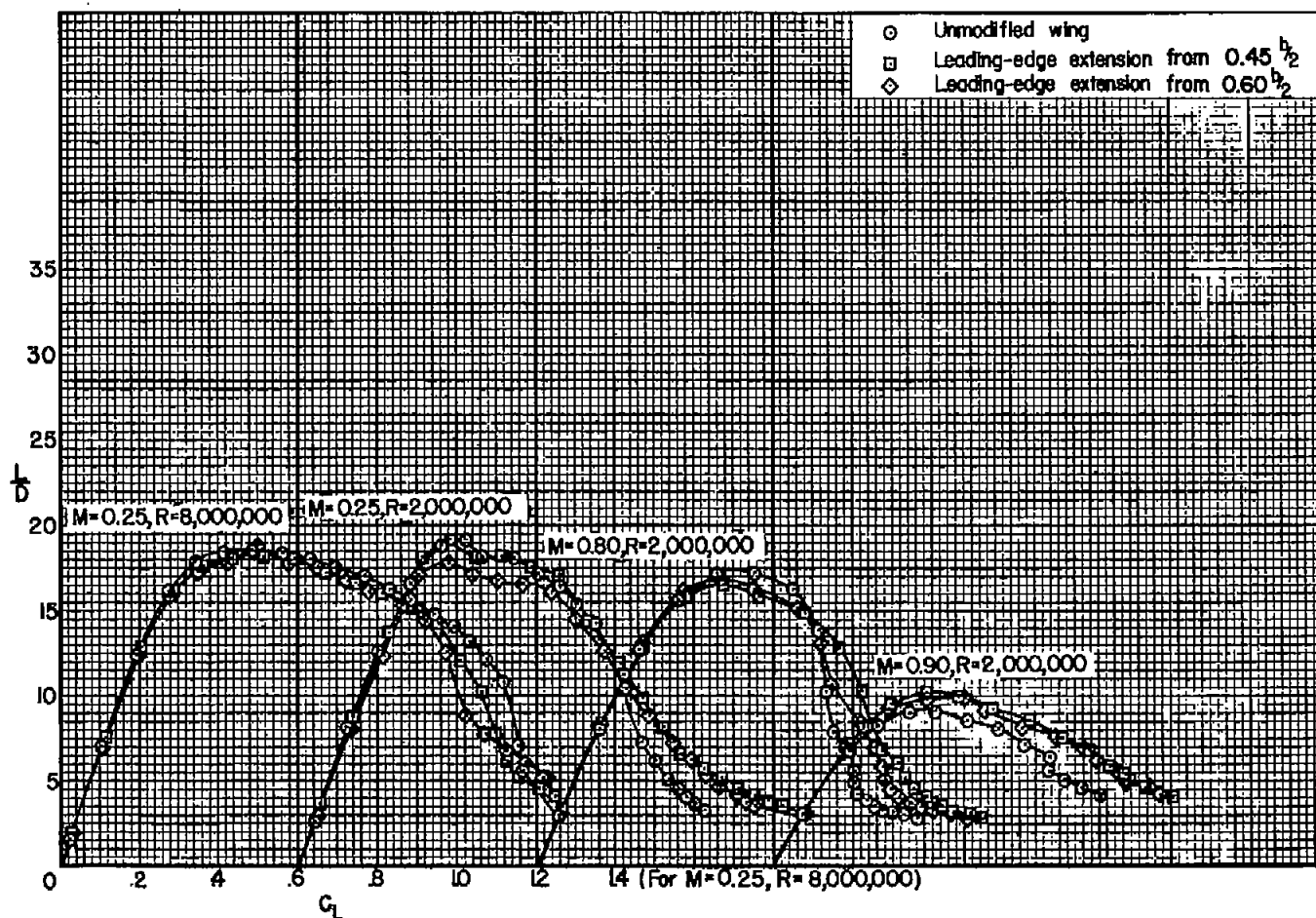
(b) Pitching moment.

Figure 11.- Continued.



(c) Drag.

Figure 11.- Continued.



(d) Lift-drag ratio.

Figure 11.- Concluded.

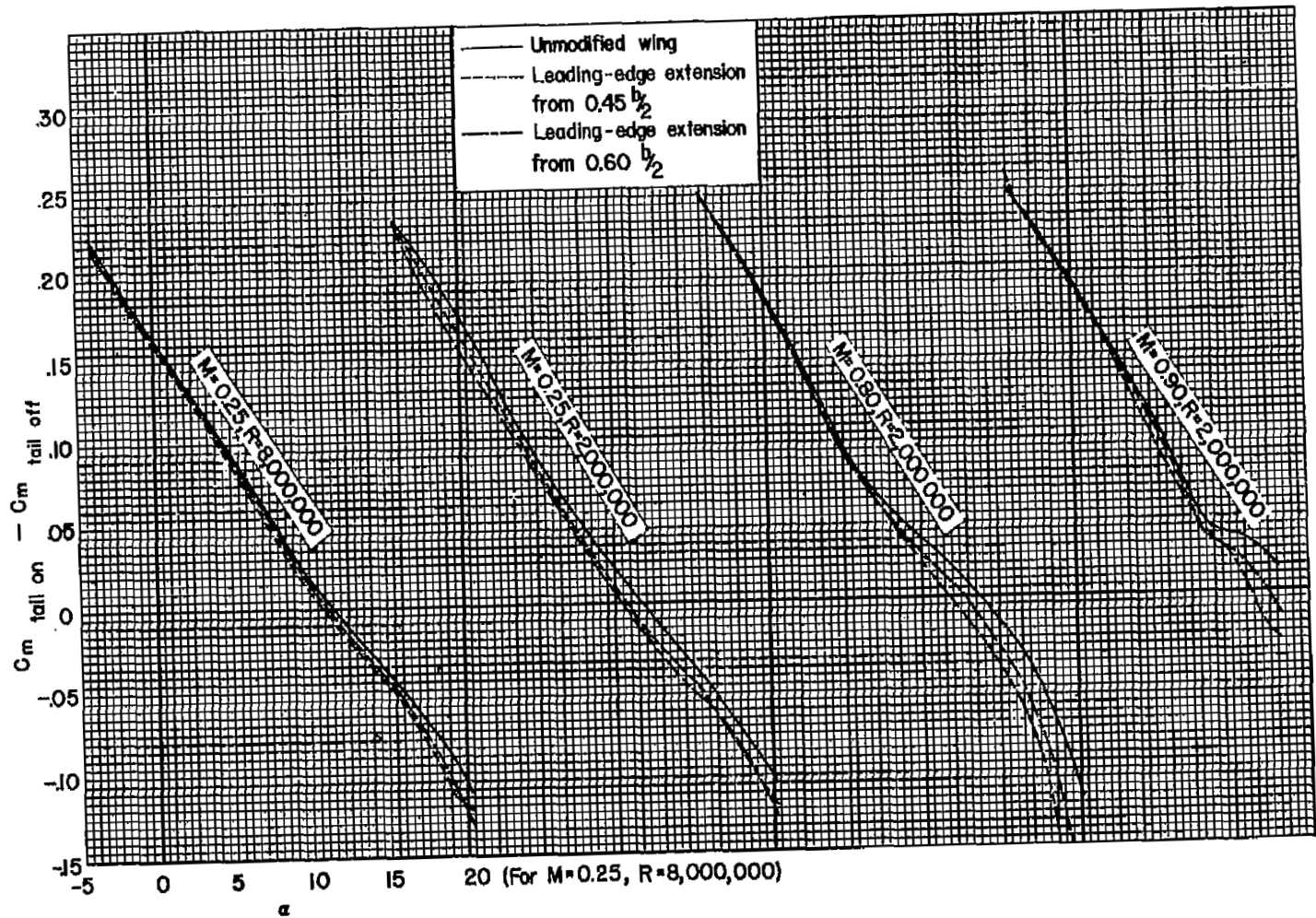


Figure 12.- The effect of leading-edge extensions on the pitching-moment contribution of the horizontal tail; $i_t = -8^\circ$.

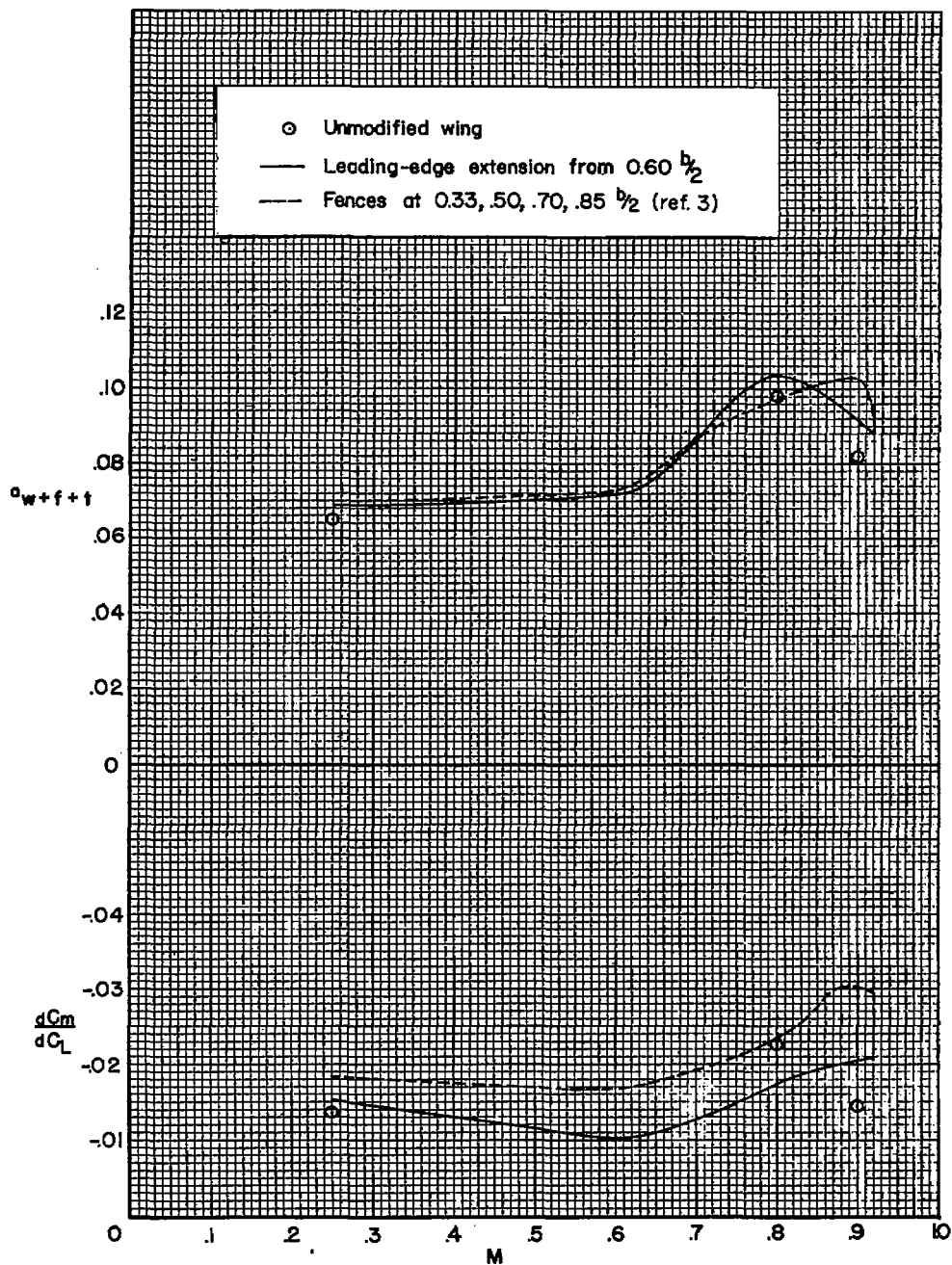


Figure 13.- The variation with Mach number of the lift and pitching-moment curve slopes of the wing-fuselage-tail combination with and without a leading edge extension and wing fences; $i_t = -8^\circ$, $C_L = 0.40$, $R = 2,000,000$.

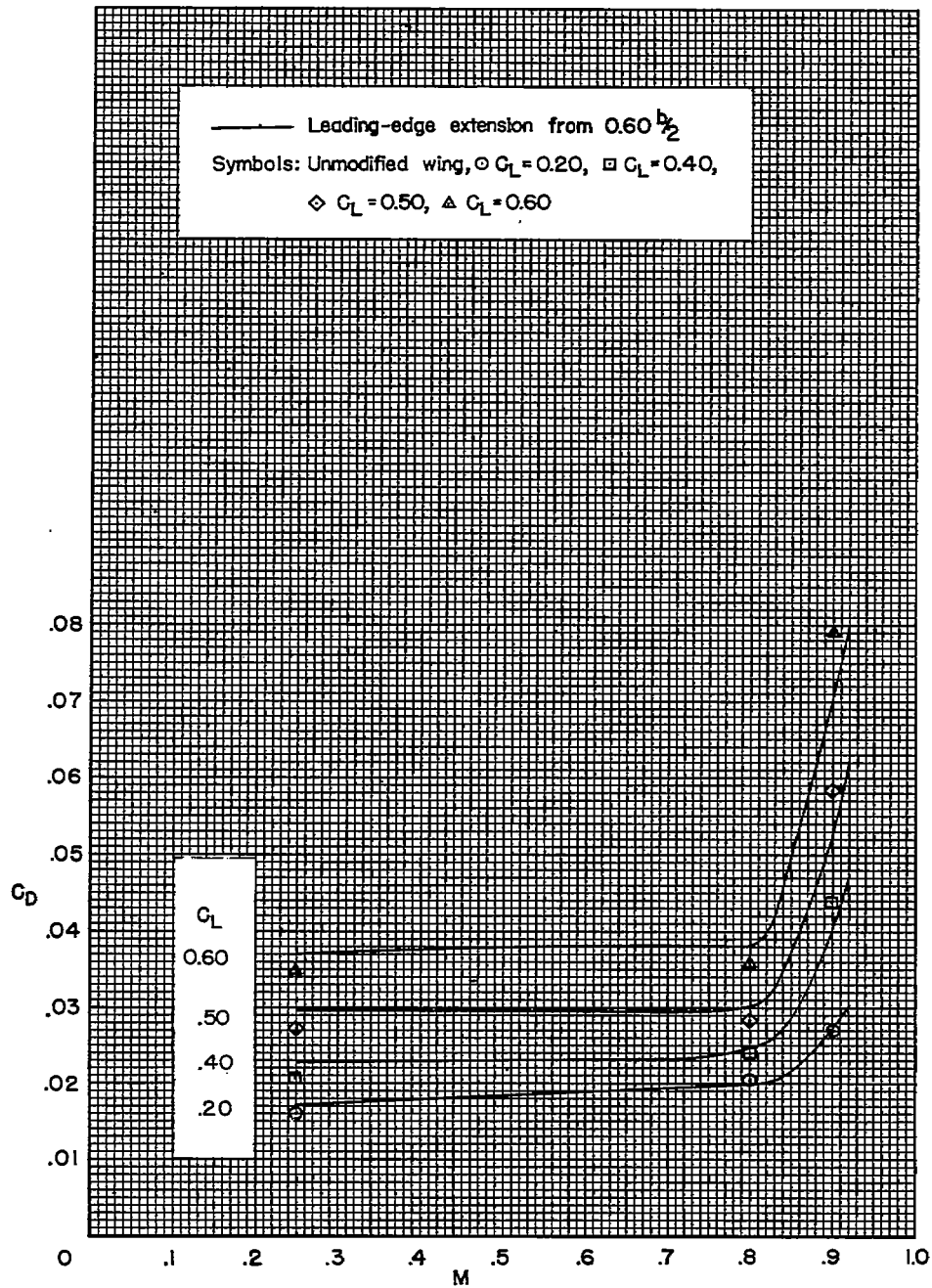
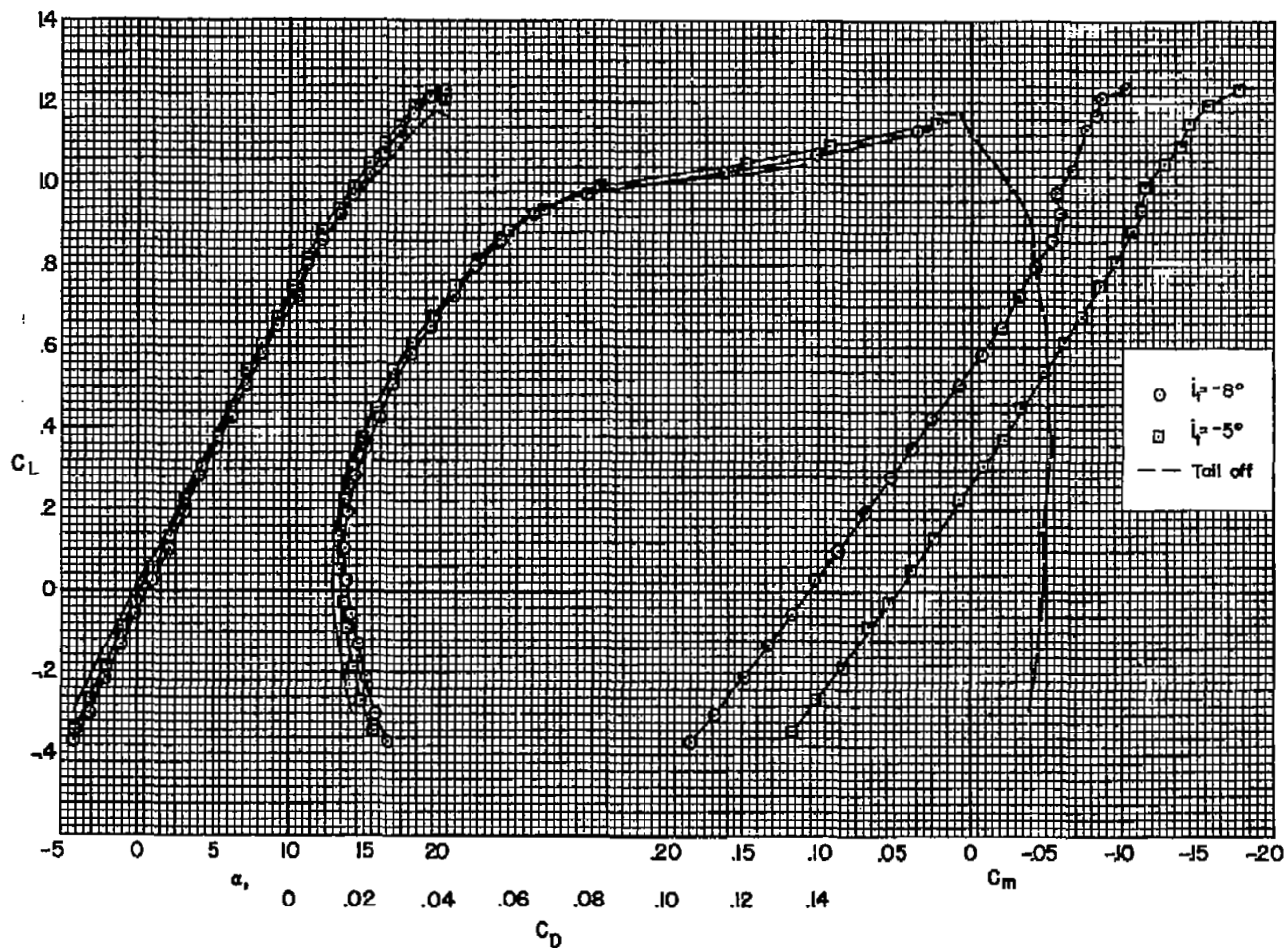
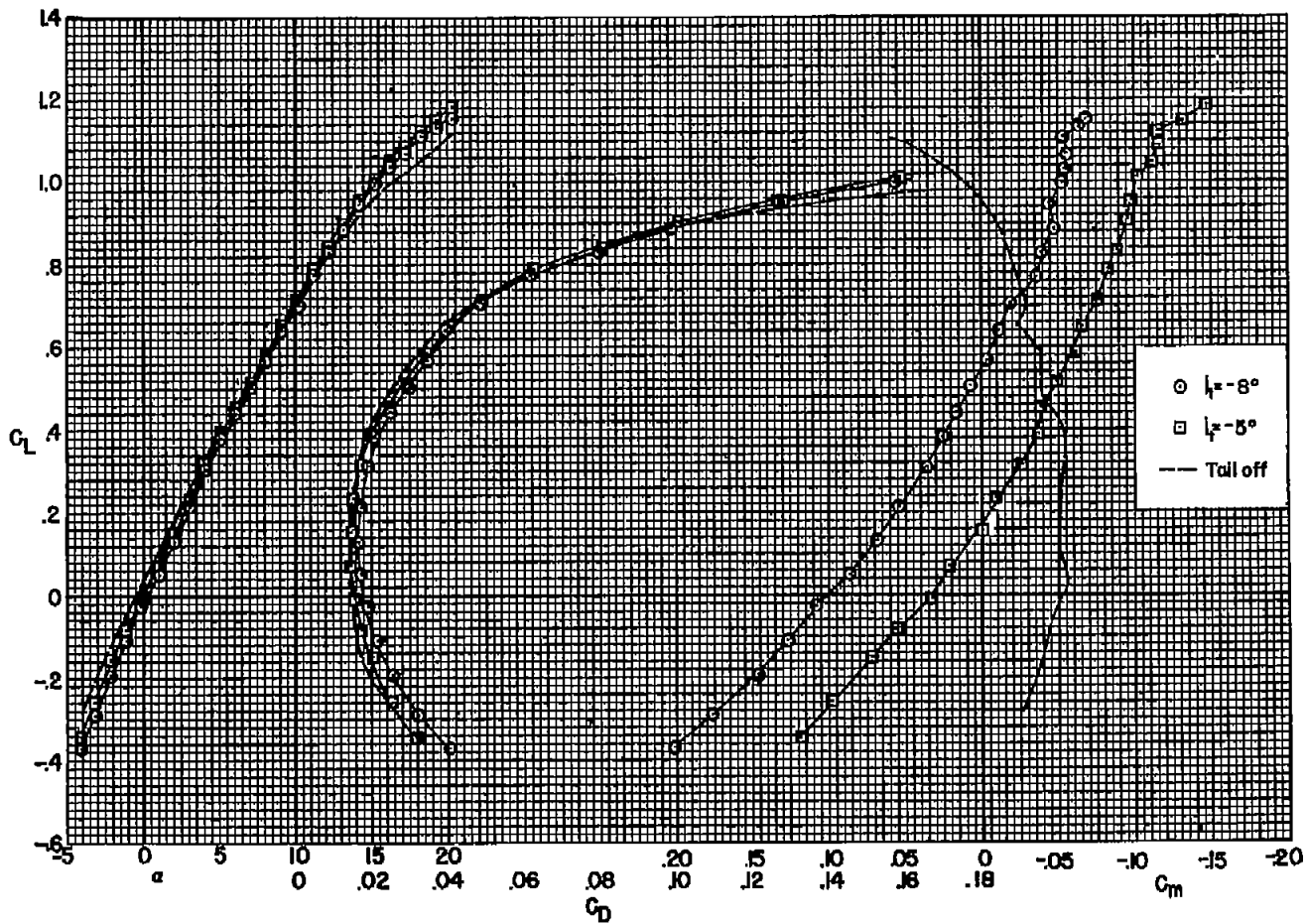


Figure 14.- The variation with Mach number of the drag coefficients of the wing-fuselage-tail combination with and without a leading-edge extension; $i_t = -8^\circ$, $R = 2,000,000$.



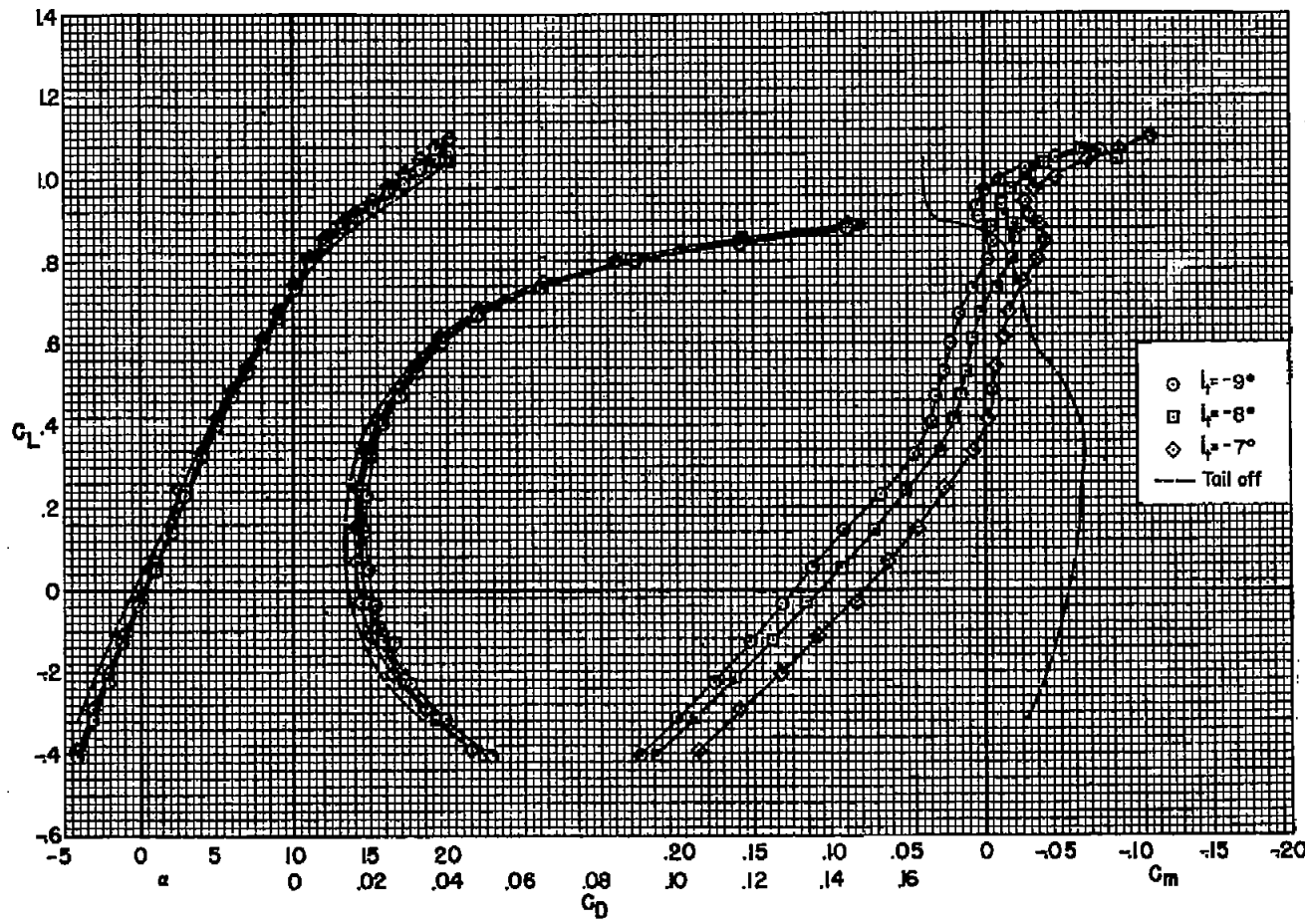
(a) $M = 0.25$, $R = 8,000,000$.

Figure 15.- The longitudinal characteristics of the combination with a leading-edge extension from 0.60 semispan to the wing tip and a horizontal tail.



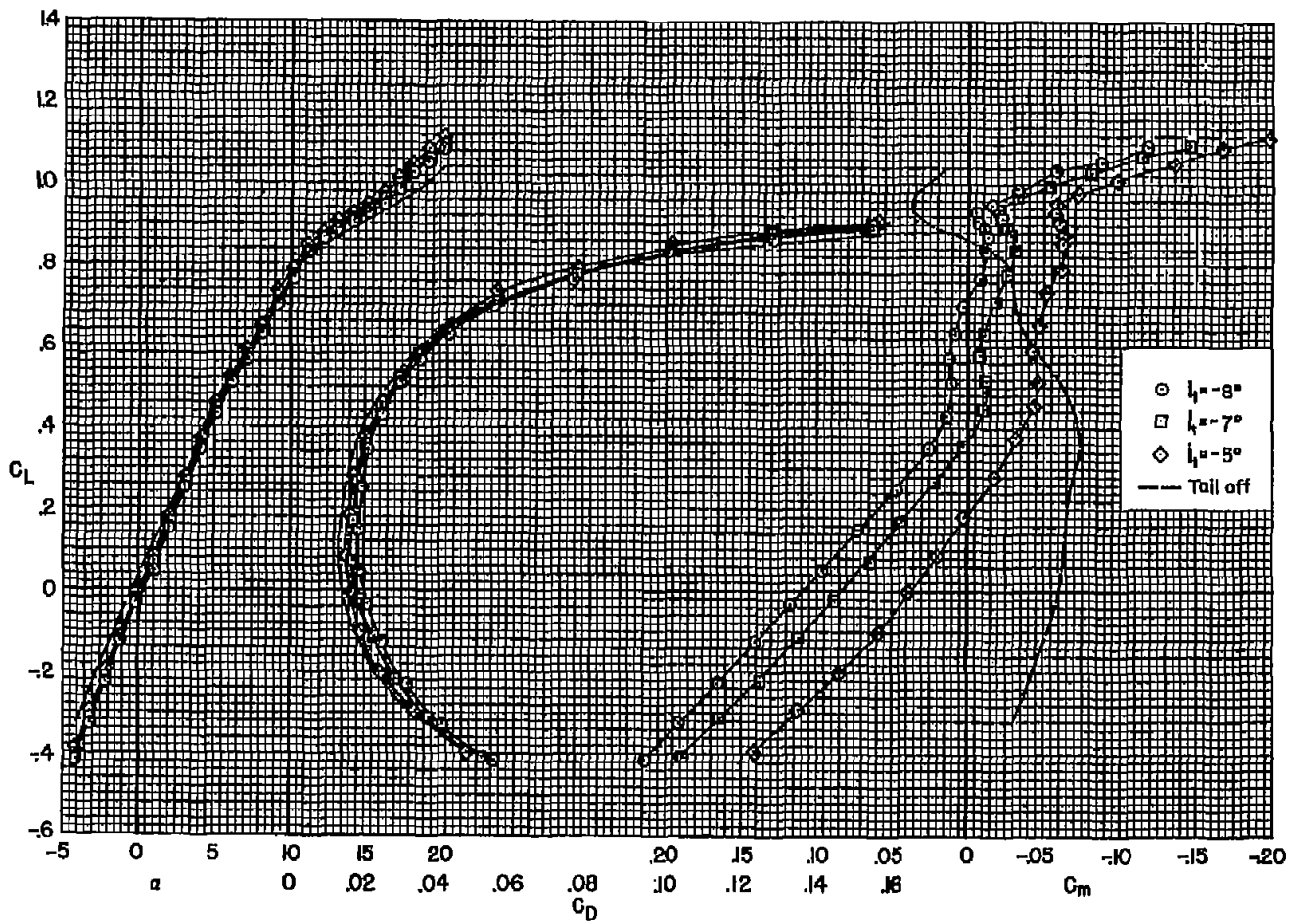
(b) $M = 0.25$, $R = 2,000,000$.

Figure 15.- Continued.



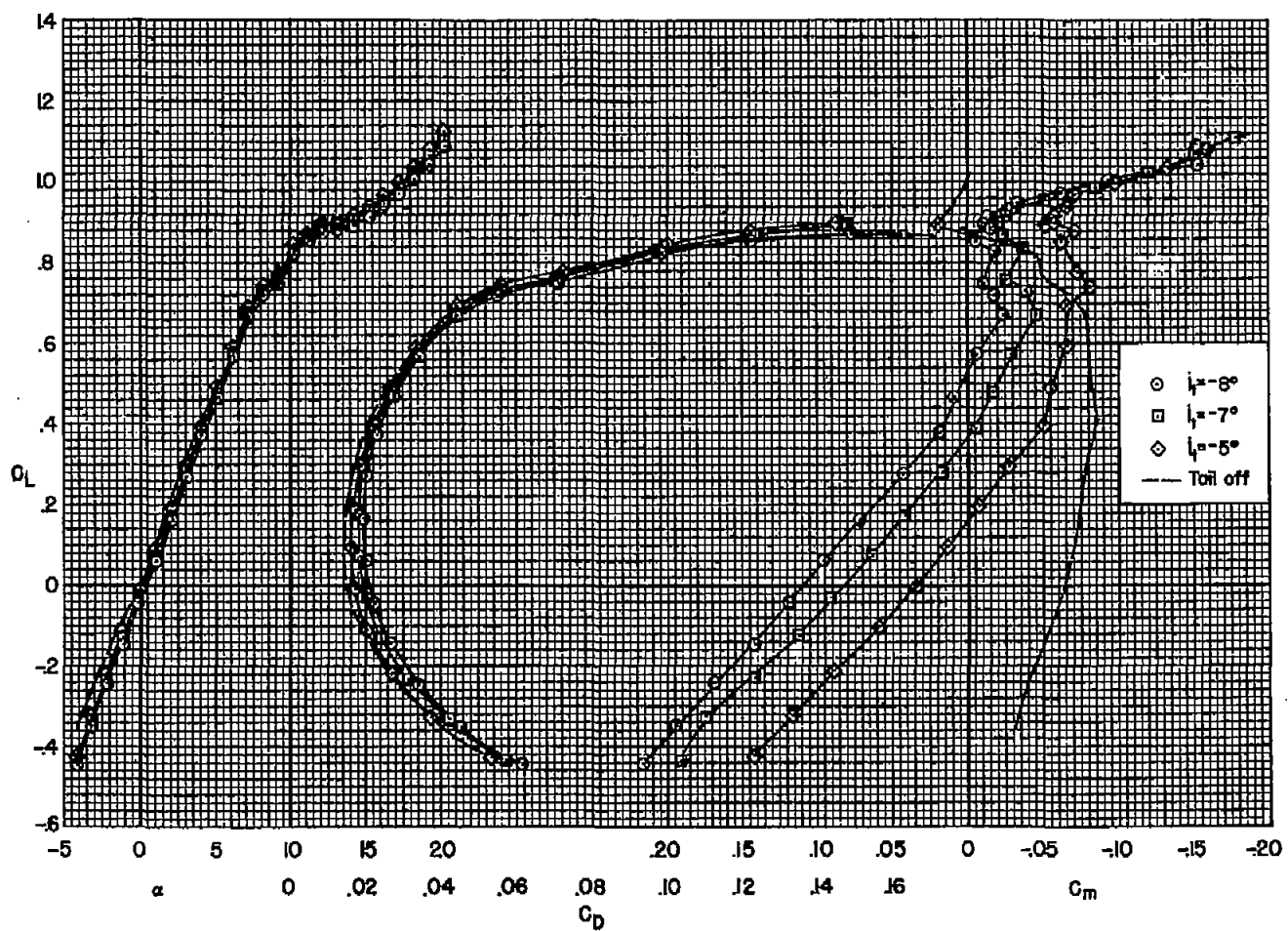
(c) $M = 0.60, R = 2,000,000.$

Figure 15.- Continued.



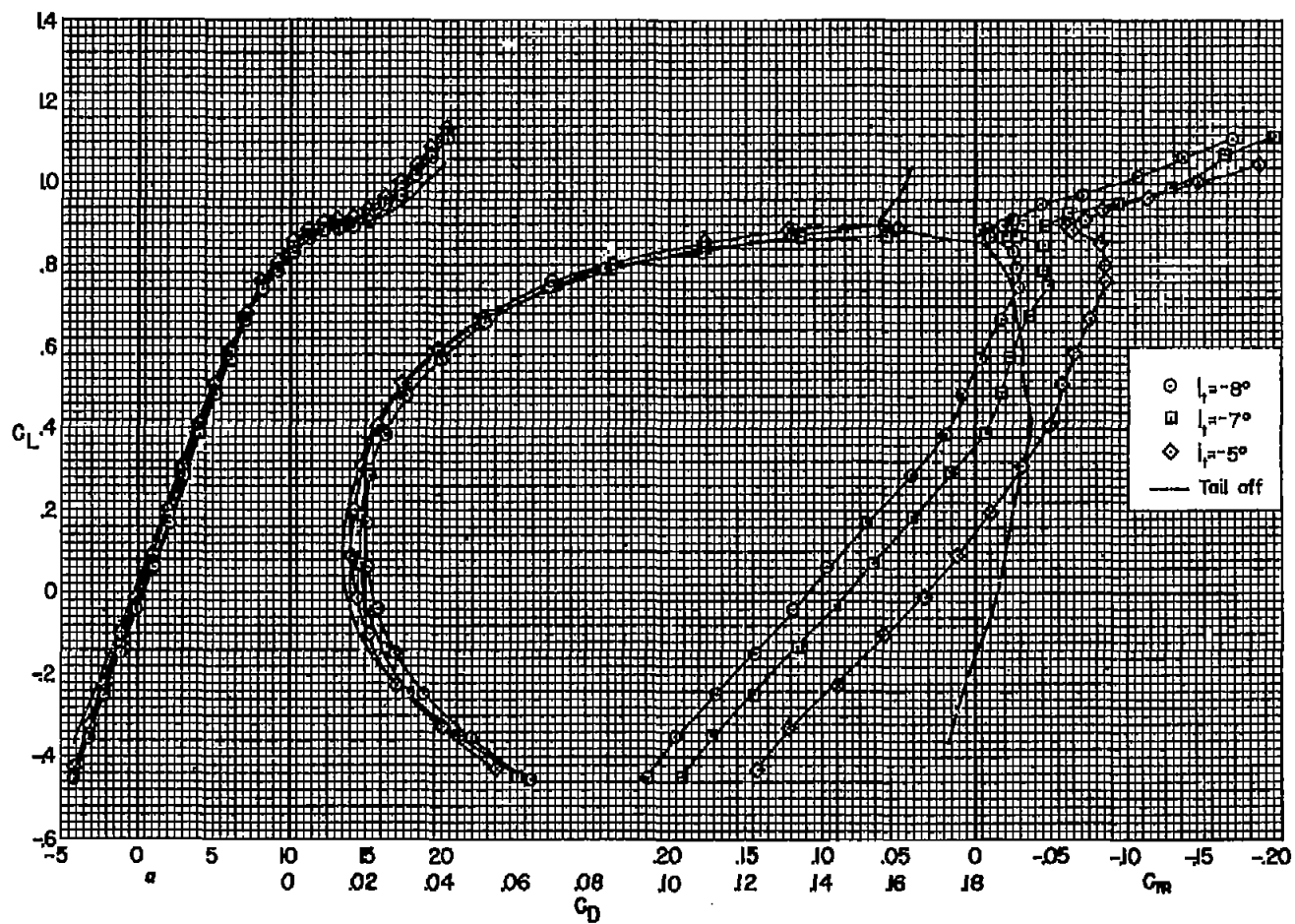
(d) $M = 0.70, R = 2,000,000.$

Figure 15.- Continued.



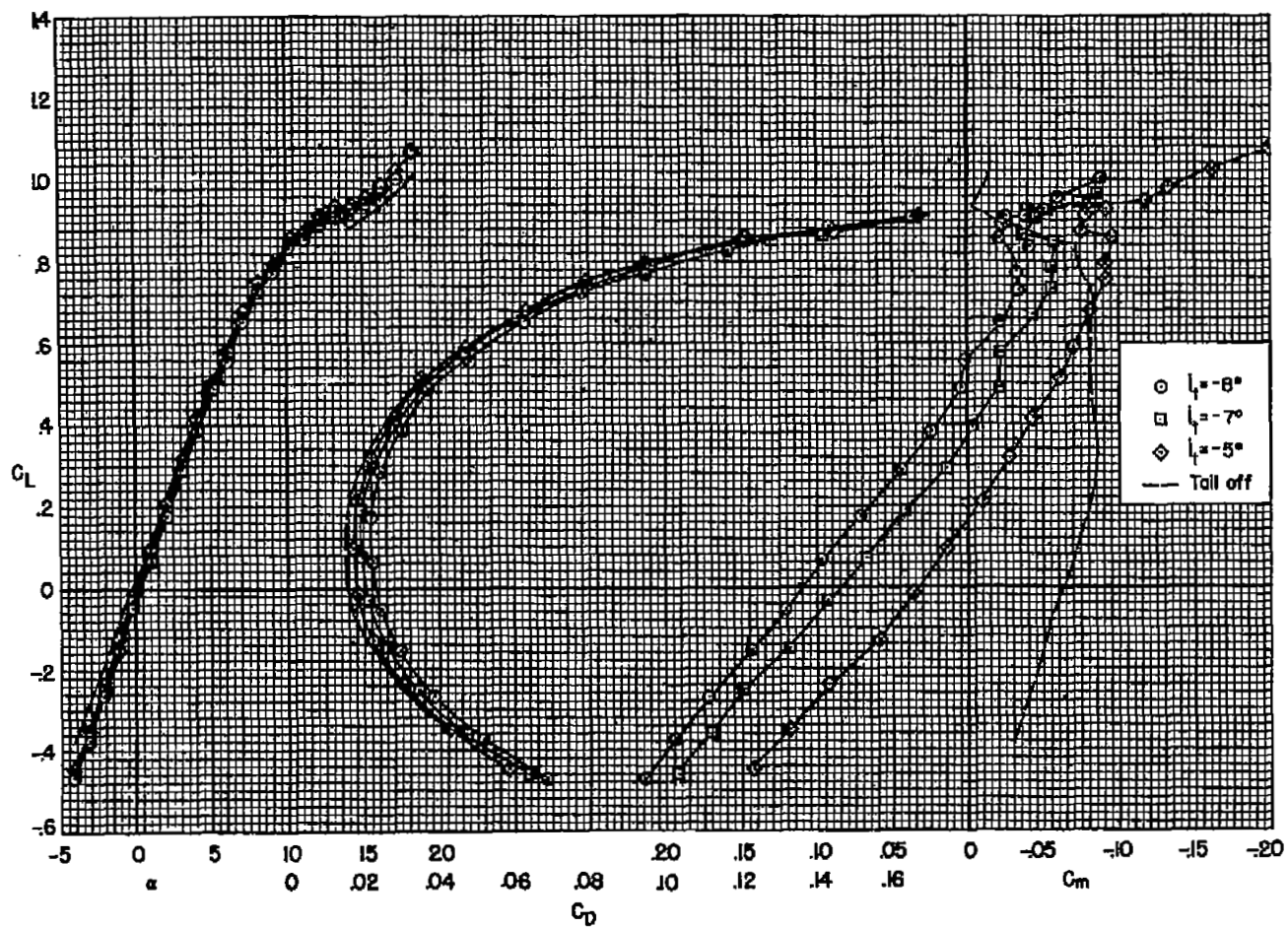
(e) $M = 0.80$, $R = 2,000,000$.

Figure 15.- Continued.



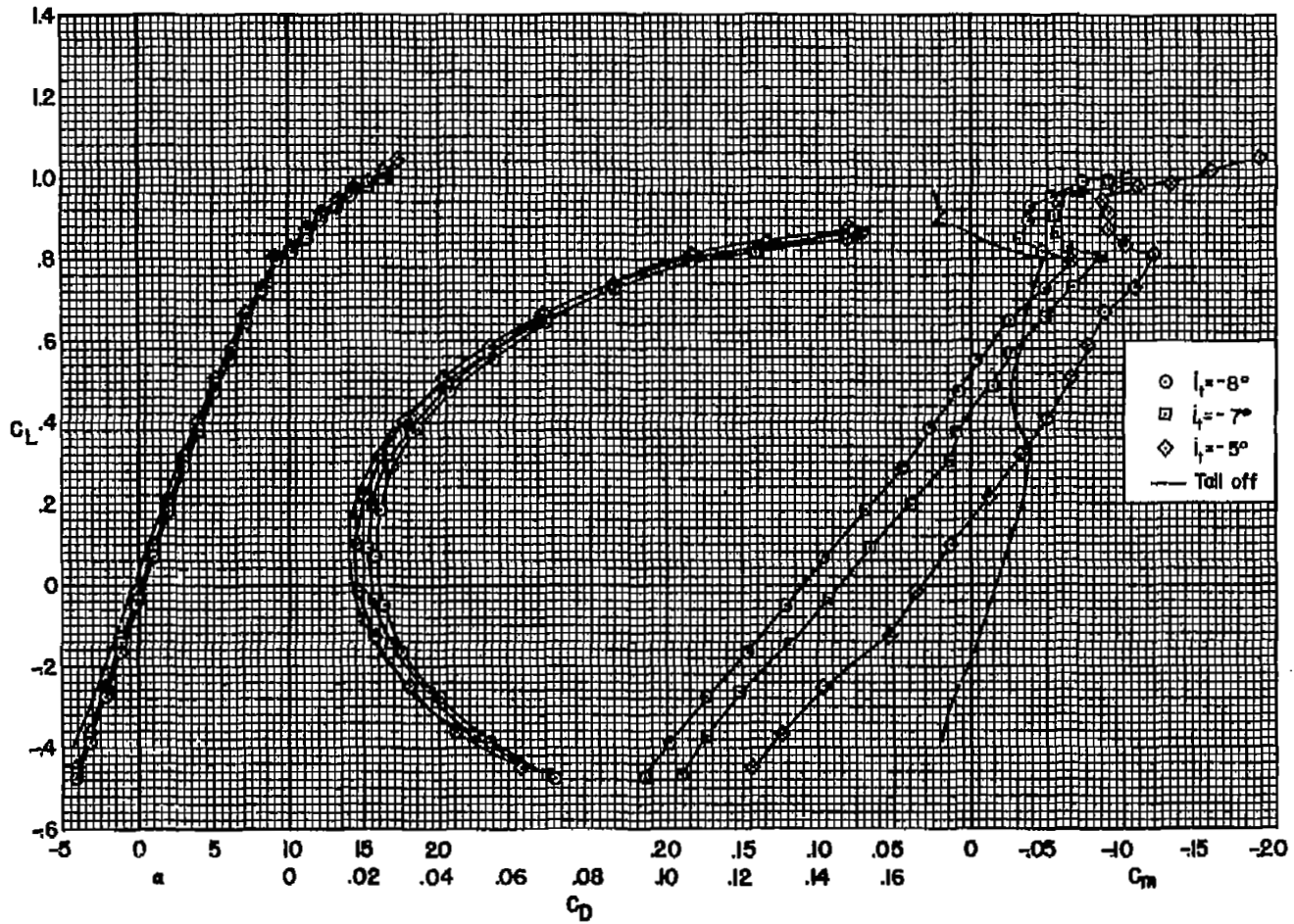
(f) $M = 0.83$, $R = 2,000,000$.

Figure 15.- Continued.



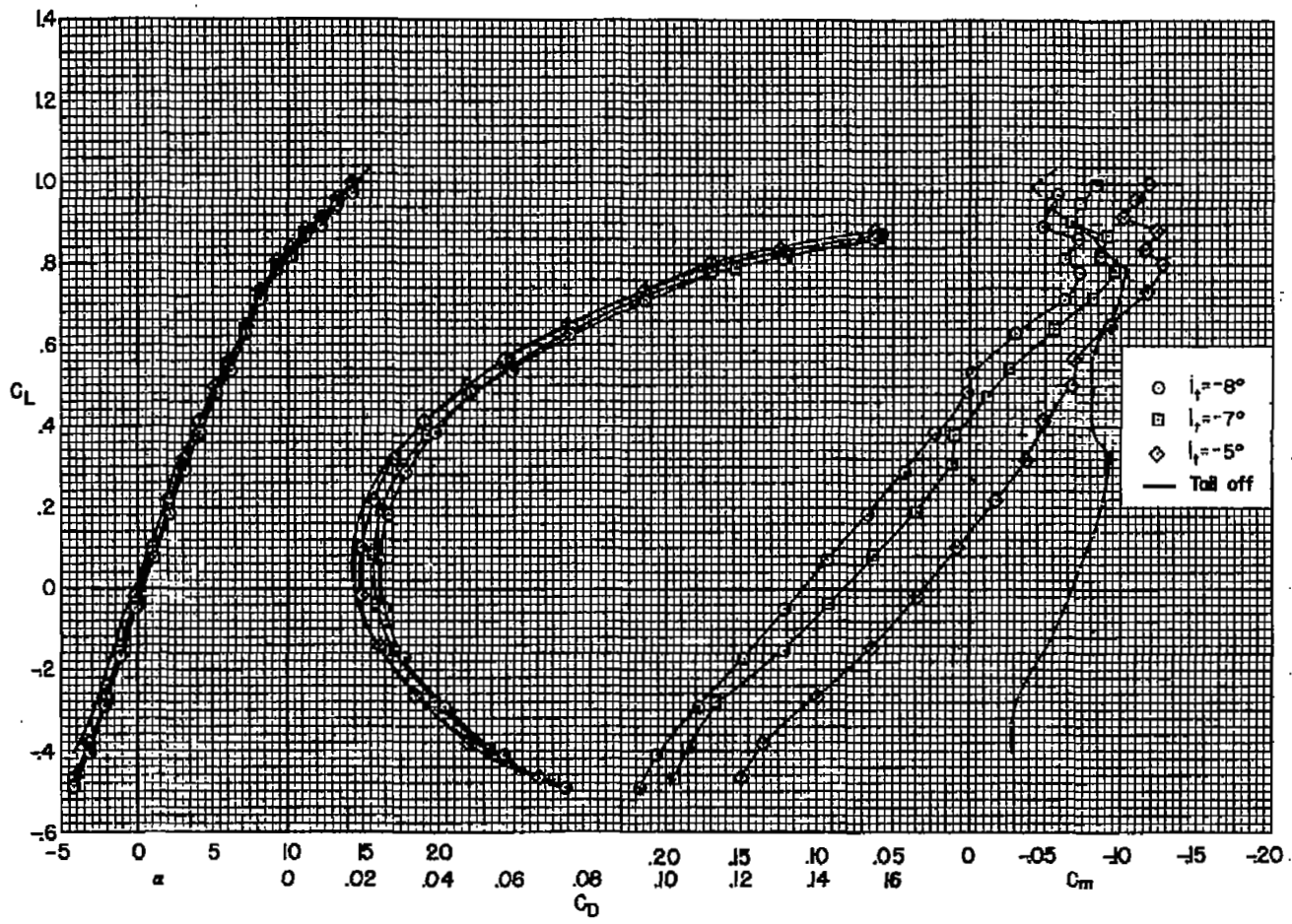
(g) $M = 0.86$, $R = 2,000,000$.

Figure 15.- Continued.



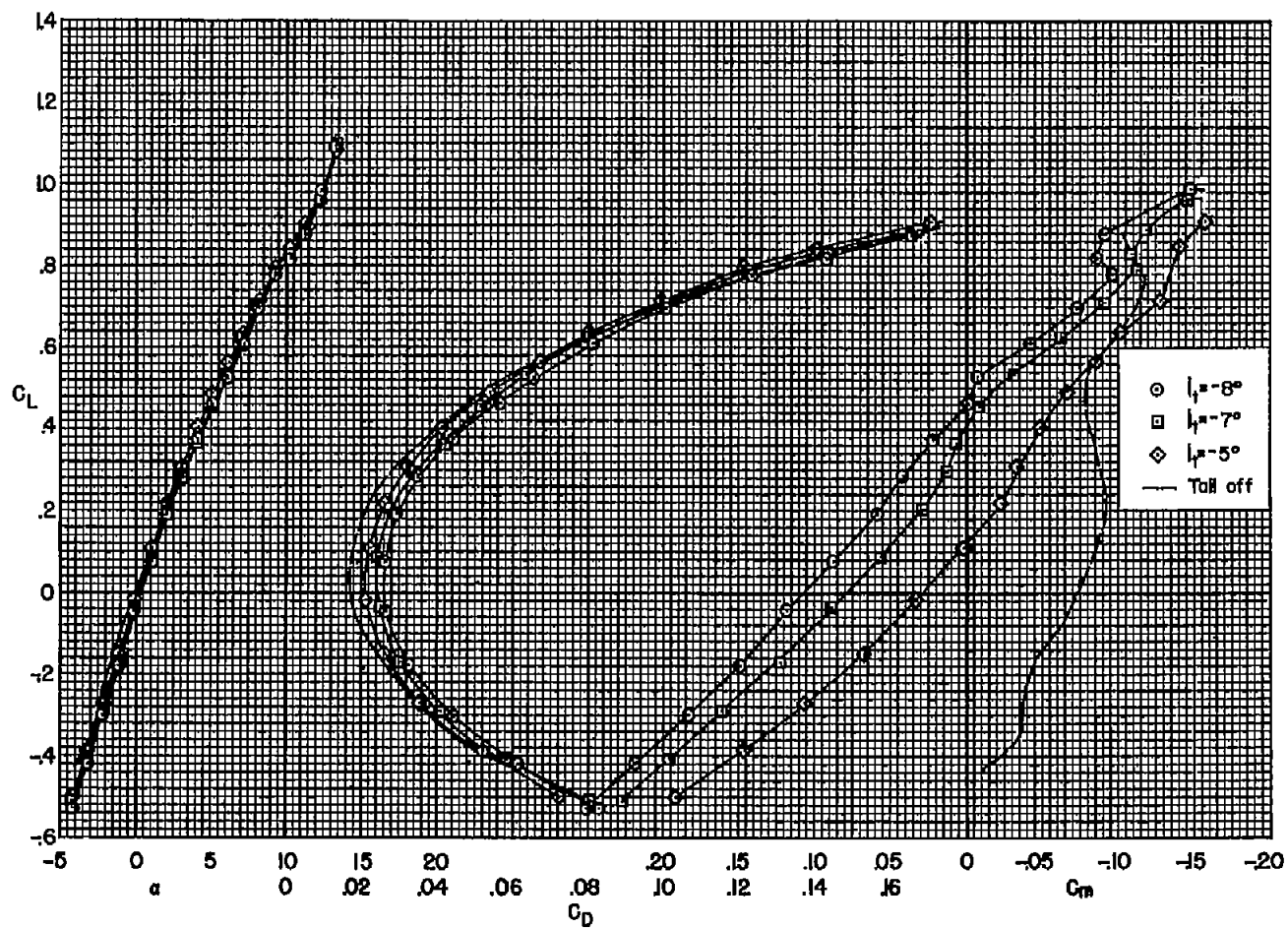
(h) $M = 0.88$, $R = 2,000,000$.

Figure 15.- Continued.



(1) $M = 0.90$, $R = 2,000,000$.

Figure 15.- Continued.



(j) $M = 0.92, R = 2,000,000.$

Figure 15.- Concluded.

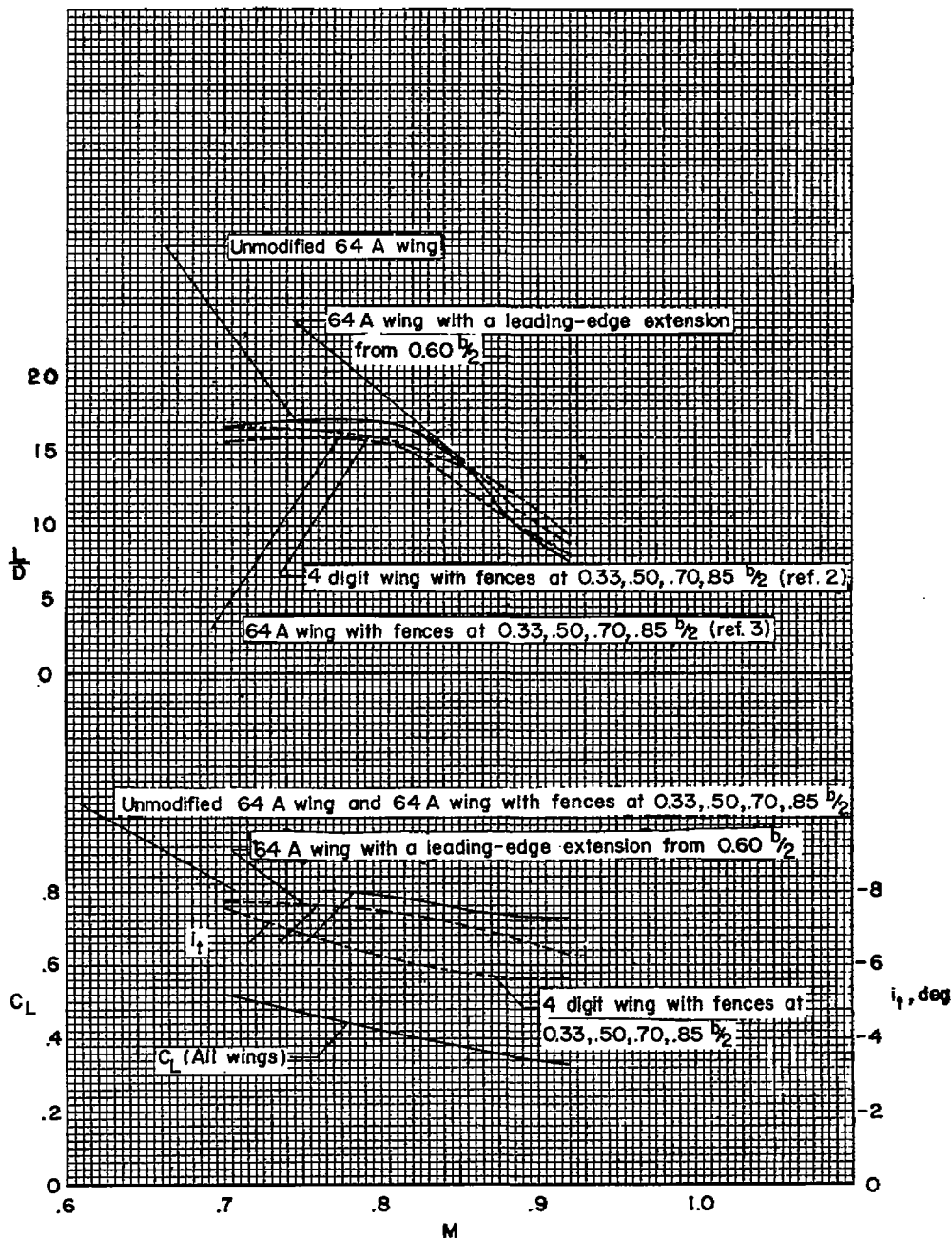


Figure 16.- The variation with Mach number of lift coefficient, tail-incidence angle, and lift-drag ratio for hypothetical airplanes in level flight at 40,000 feet; $W/S = 75$ pounds per square foot.

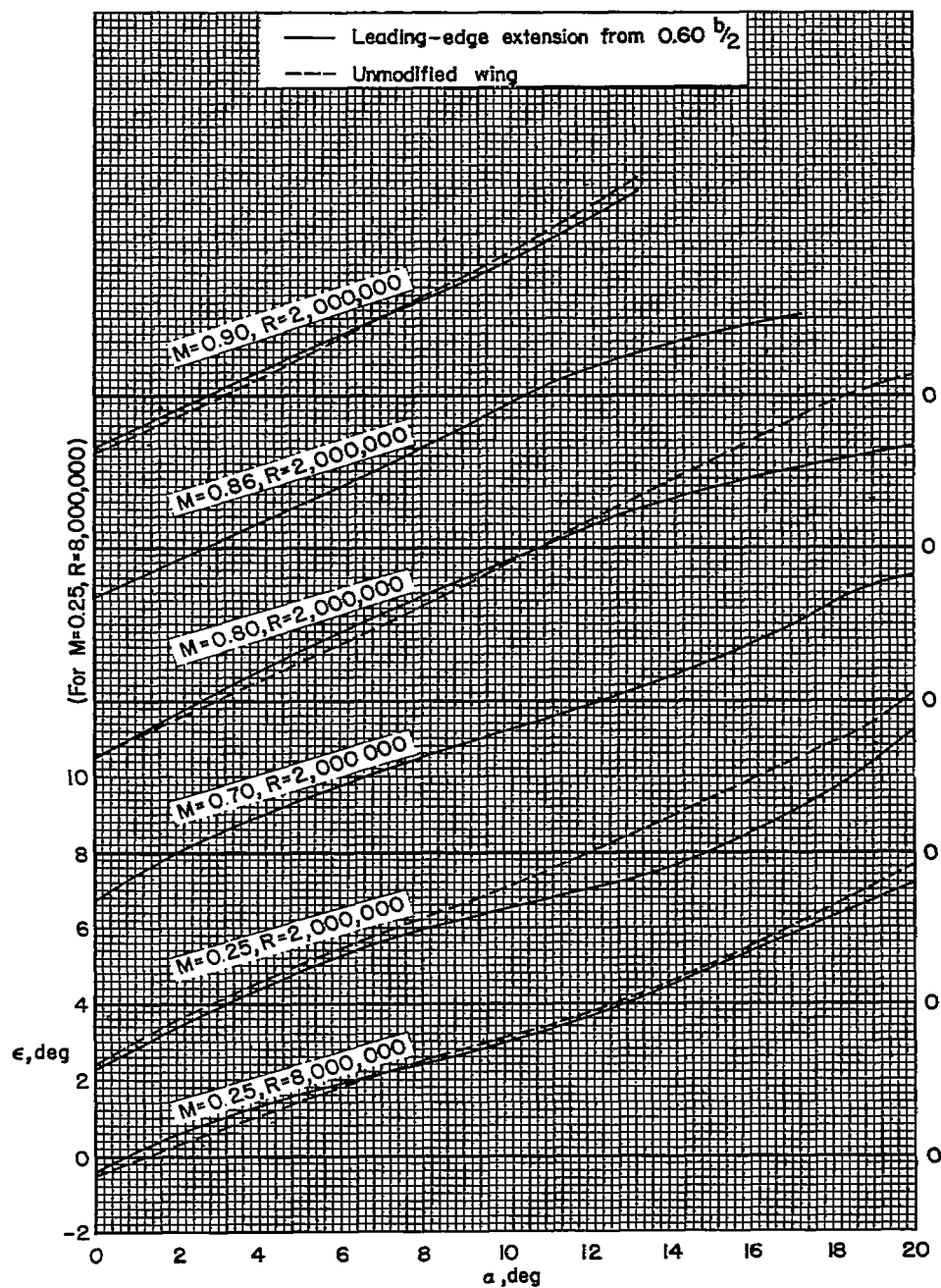
(a) ϵ vs. α

Figure 17.- The variation with angle of attack of the factors affecting the stability contribution of the horizontal tail.

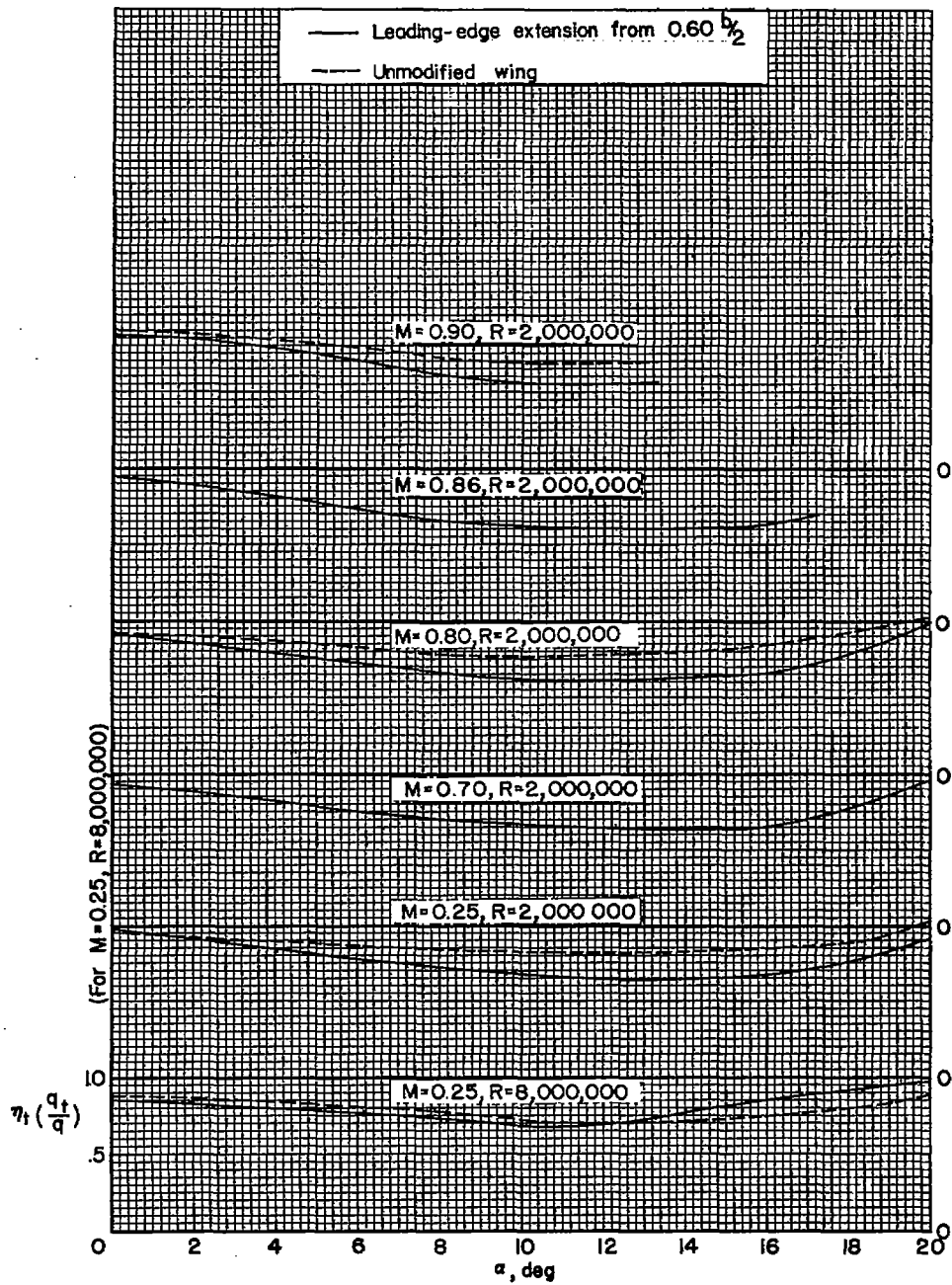
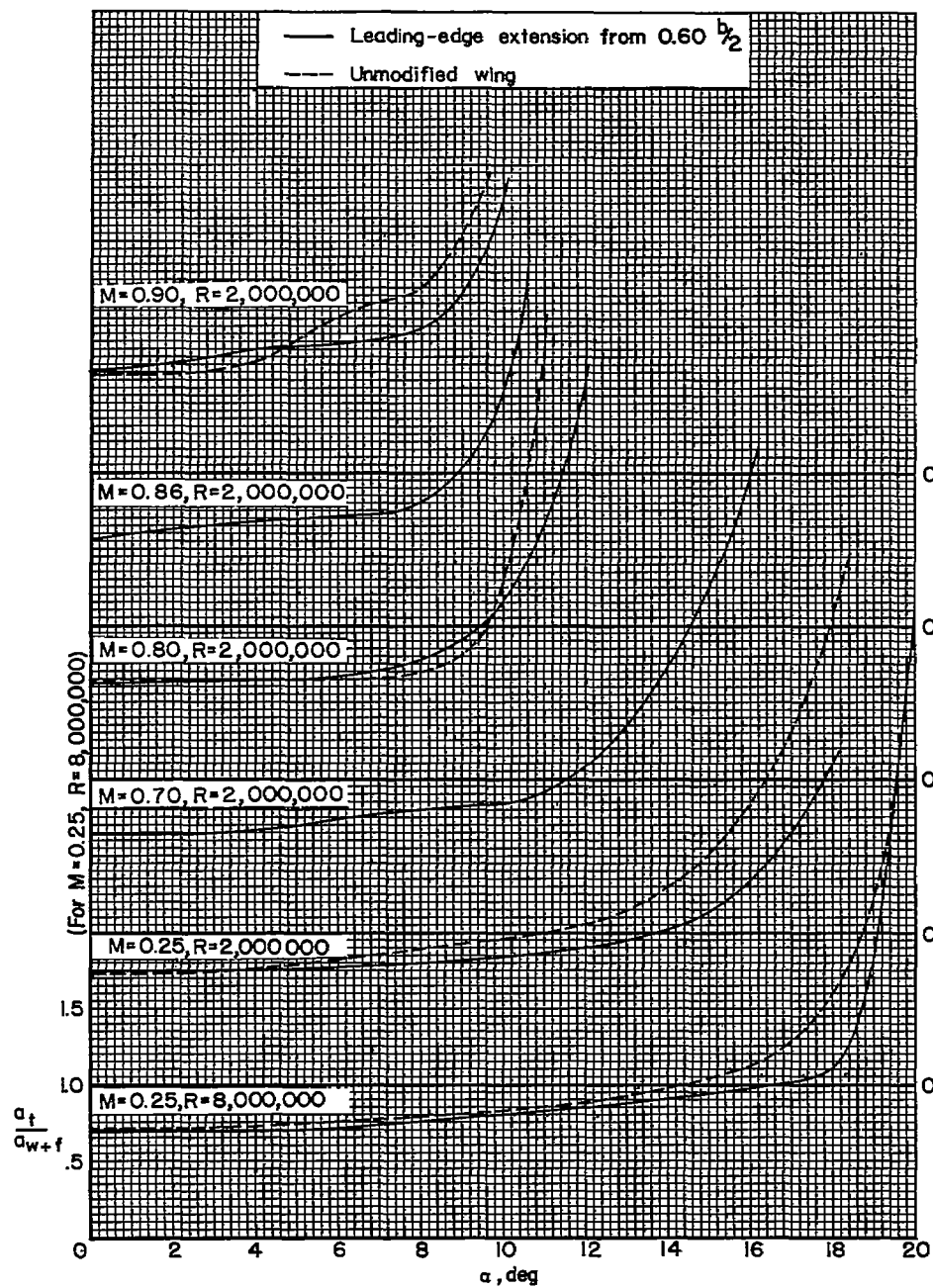
(b) $\eta_t(q_t/q)$ vs. α

Figure 17.- Continued.



(c) a_t/a_{w+f} vs. α

Figure 17.- Concluded.

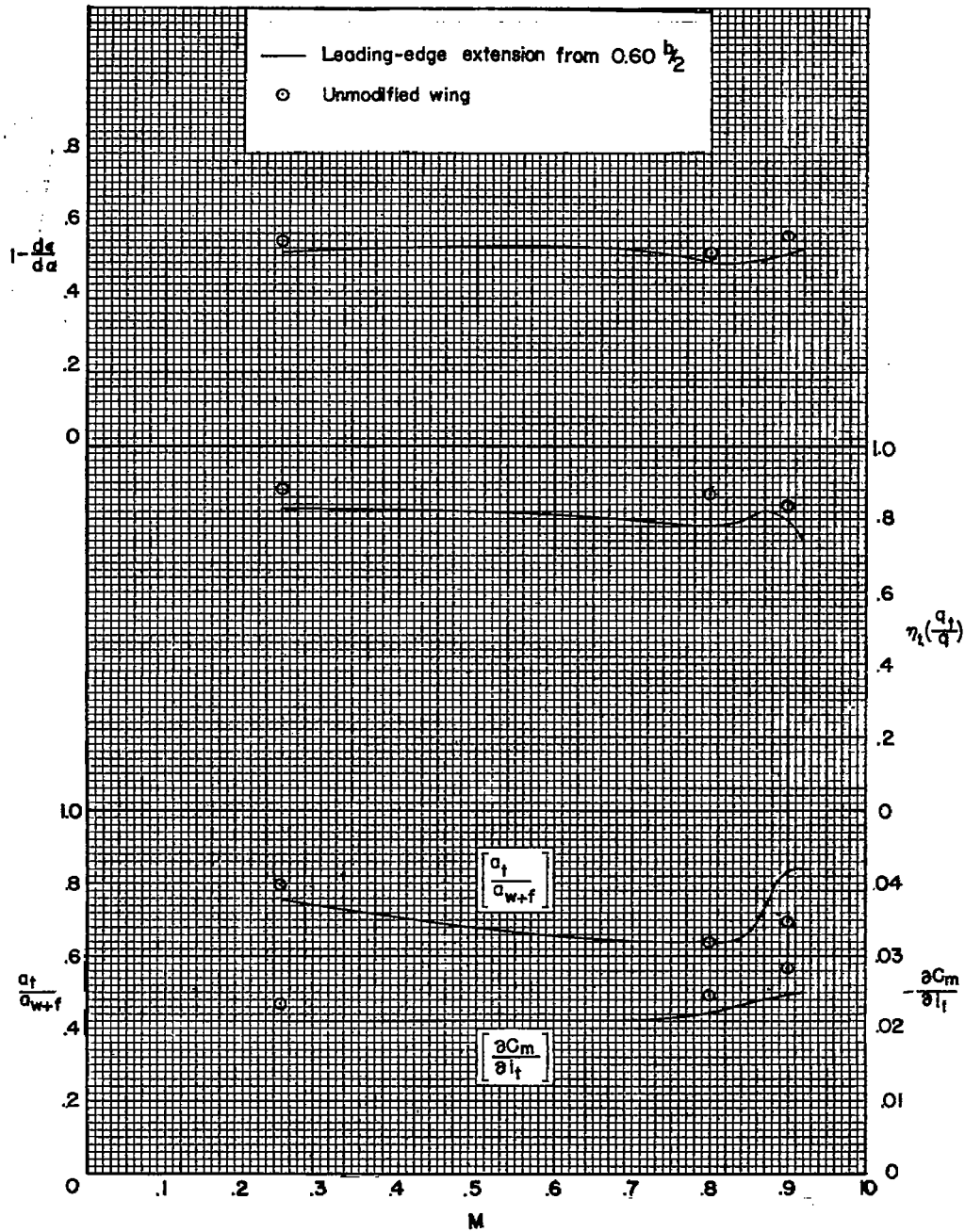


Figure 18.- The variation with Mach number of the control effectiveness and the factors affecting the stability contribution of the horizontal tail; $\alpha = 4^\circ$, $R = 2,000,000$.



3 1176 01434 8578

